



Deposited via The University of Leeds.

White Rose Research Online URL for this paper:

<https://eprints.whiterose.ac.uk/id/eprint/144776/>

Version: Accepted Version

Article:

Ely, JC, Clark, CD, Hindmarsh, RCA et al. (2021) Recent progress on combining geomorphological and geochronological data with ice sheet modelling, demonstrated using the last British–Irish Ice Sheet. *Journal of Quaternary Science*, 36 (5). pp. 946-960. ISSN: 0267-8179

<https://doi.org/10.1002/jqs.3098>

© 2019 John Wiley & Sons, Ltd. This is the peer reviewed version of the following article: Ely, J. C., Clark, C. D., Hindmarsh, R. C., Hughes, A. L., Greenwood, S. L., Bradley, S. L., Gasson, E., Gregoire, L., Gandy, N., Stokes, C. R. and Small, D. (2019), Recent progress on combining geomorphological and geochronological data with ice sheet modelling, demonstrated using the last British–Irish Ice Sheet. *J. Quaternary Sci.*, which has been published in final form at <https://doi.org/10.1002/jqs.3098>. This article may be used for non-commercial purposes in accordance with Wiley Terms and Conditions for Use of Self-Archived Versions.

Reuse

Items deposited in White Rose Research Online are protected by copyright, with all rights reserved unless indicated otherwise. They may be downloaded and/or printed for private study, or other acts as permitted by national copyright laws. The publisher or other rights holders may allow further reproduction and re-use of the full text version. This is indicated by the licence information on the White Rose Research Online record for the item.

Takedown

If you consider content in White Rose Research Online to be in breach of UK law, please notify us by emailing eprints@whiterose.ac.uk including the URL of the record and the reason for the withdrawal request.

1 **Recent progress on combining geomorphological and geochronological data with ice**
2 **sheet modelling, demonstrated using the last British-Irish Ice Sheet**

3
4 Jeremy C. Ely¹, Chris D. Clark¹, Richard C.A. Hindmarsh², Anna L.C. Hughes³, Sarah L.
5 Greenwood⁴, Sarah L. Bradley⁵, Edward Gasson⁶, Lauren Gregoire⁷, Niall Gandy⁷, Chris R.
6 Stokes⁸ and David Small⁸.

7
8 1 – Department of Geography, The University of Sheffield, Sheffield, S10 2TN, UK

9 2 – British Antarctic Survey, High Cross, Madingley Road, Cambridge, CB3 0ET, UK

10 3 - Department of Earth Science, University of Bergen and Bjerknes Centre for Climate
11 Research, Bergen, Norway

12 4 - Department of Geological Sciences, Stockholm University, Stockholm, Sweden

13 5 - Department of Geoscience and Remote Sensing, Delft University of Technology,
14 Stevinweg 1, 2628 CN Delft, Netherlands

15 6 – School of Geographical Sciences, University of Bristol, University Road, Bristol, BS8
16 1SS, UK

17 7 - University of Leeds, School of Earth and Environment, Woodhouse Lane, Leeds, LS2
18 9JT, UK

19 8 – Durham University, Department of Geography, Lower Mountjoy, South Road, Durham,
20 DH1 3LE, UK

21
22 **Abstract**

23 Palaeo-ice sheets are important analogues for understanding contemporary ice sheets,
24 offering a record of ice sheet behaviour that spans millennia. There are two main approaches
25 to reconstructing palaeo-ice sheets. Empirical reconstructions use the available glacial
26 geological and chronological evidence to estimate ice sheet extent and dynamics but lack
27 direct consideration of ice physics. In contrast, numerically-modelled simulations implement
28 ice physics, but often lack direct quantitative comparison to empirical evidence. Despite
29 being long-identified as a fruitful scientific endeavour, few ice sheet reconstructions attempt
30 to reconcile the empirical and model-based approaches. To achieve this goal, model-data
31 comparison procedures are required. Here, we compare three numerically-modelled
32 simulations of the former British-Irish Ice Sheet with the following lines of evidence: (i)

33 position and shape of former margin positions, recorded by moraines; (ii) former ice-flow
34 direction and flow-switching, recorded by flowsets of subglacial bedforms; and (iii), the
35 timing of ice-free conditions, recorded by geochronological data. These model-data
36 comparisons provide a useful framework for quantifying the degree of fit between numerical
37 model simulations and empirical constraints. Such tools are vital for reconciling numerical
38 modelling and empirical evidence, the combination of which will lead to more robust palaeo-
39 ice sheet reconstructions with greater explicative and ultimately predictive power.

40

41 **1. Introduction**

42 Reconstructing the behaviour of palaeo-ice sheets enables a better understanding of the
43 long-term (centennial to millennial) behaviour of ice sheets in the Earth system. The former
44 extent and behaviour of ice sheets can be inferred principally from four main lines of
45 evidence. First, relative sea-level (RSL) records (e.g. a raised beach or salt marsh) provide
46 constraints on the loading history of an ice sheet. Through the application of a glacio-isostatic
47 adjustment (GIA) model, RSL data can be used to infer palaeo-ice sheet thickness and extent
48 (e.g. Lambeck and Chappell, 2001; Peltier, 2004; Bradley et al., 2011). Secondly, analysis of
49 the properties and stratigraphic sequence of sediments transported and deposited by palaeo-
50 ice sheets can be used to infer ice sheet history at a given location (e.g. Eyles and McCabe,
51 1989; Piotrowski and Tulaczyk, 1999). The geomorphological record, composed of
52 landforms such as drumlins and moraines, can be used to decipher former ice-flow directions
53 and margin positions (e.g. Hughes et al., 2014; Clark et al., 2018). Finally, the timing of
54 deposition of sediment and/or the time glacially transported or eroded bedrock has been
55 exposed, and by inference the timing of formation of associated landforms, can be dated
56 using laboratory-based techniques to produce the third line of evidence, geochronological
57 data (e.g. Libby et al., 1949; Duller, 2006; Small et al., 2017a).

58 The body of empirical evidence related to palaeo-ice sheets is continually growing,
59 producing an ever-expanding library of palaeo-ice sheet data (e.g. Dyke, 2004; Clark et al.,
60 2012; Hughes et al., 2016; Stroeven et al., 2016). Producing a glaciologically-plausible
61 *empirical reconstruction* of a palaeo-ice sheet is, however, a challenging process, with three
62 main limitations. First, evidence is often temporally and spatially fragmented, thereby
63 requiring some subjective inference to be made about ice sheet behaviour between the data-
64 constraints (Clark et al., 2012; Hughes et al., 2016). Secondly, all sources of data have

65 inherent uncertainties due to factors such as preservation potential, inherent laboratory-based
66 uncertainties and post-depositional modification (Hughes et al., 2016; Small et al., 2017a).
67 Finally, a mathematically- and physically-based direct inversion from palaeo-glaciological
68 information to infer past-ice sheet characteristics (e.g. former ice-flow velocities) has
69 remained elusive owing to the complexity of processes involved, meaning that all
70 reconstructions are subjective (albeit expert) inferences (Kleman and Borgström, 1996;
71 Stokes et al., 2015). Despite these limitations, empirical reconstructions typically provide a
72 spatially-coherent representation of ice sheet activity, often portrayed as a series of
73 palaeogeographic maps showing ice extent, flow geometry, ice divides and their changes at
74 any given time (or at several time-steps).

75 As an alternative to the data-driven approach of an empirical reconstruction, numerical
76 ice sheet models can be used to reconstruct palaeo-ice sheet behaviour (e.g. Fisher et al.,
77 1985; Tarasov and Peltier, 2004; Hubbard et al., 2009; Patton et al., 2017). The approach here
78 is to apply a numerical model based on the understanding of ice sheet physics to produce a
79 *modelled reconstruction* of a palaeo-ice sheet. Using this physics-based approach,
80 information such as ice-thickness and velocity can be reconstructed across the entire model
81 domain in a manner that is consistent with model physics. However, limitations with this
82 approach mean that modelled reconstructions may struggle to replicate the information and
83 detail provided by palaeo-data. Numerical ice sheet models require the specification of
84 several input boundary conditions and parameters. One of the most uncertain of these is the
85 climatic conditions used to determine the pattern of accumulation and ablation over the
86 model domain through time (Stokes et al., 2015). Other factors relating to the nature of ice
87 sheet flow, such as basal friction, subglacial hydrology and shear, may either rely upon
88 poorly constrained model parameters (due to a lack of physical understanding), or simply be
89 beyond the capabilities of the model (e.g. they operate at scales below the spatial resolution
90 of the model). Compounding the problem, ice sheets exhibit instabilities, whereby small
91 perturbations to boundary conditions are amplified by the instability and can affect the whole
92 modelled ice sheet. Such instabilities may lead to highly non-linear responses that are
93 difficult to predict. One example is the marine ice sheet instability (Hughes, 1973; Schoof,
94 2007; 2012), which is an instability in the position of the grounding-line on a reverse bed
95 slope that occurs as a consequence of ice-flux being proportional to ice-thickness at the
96 grounding-line.

97 A complementary approach to the above is to view ice sheet behaviour as an expression
98 of the weather/climate duality; “climate is what on an average we expect, weather is what we
99 actually get” (Herbertson, 1908, p. 118). Restricting our attention to NW Europe, over diurnal
100 periods weather is quite predictable, but this statement is false over time periods of a few
101 days. On the other hand, it is true to say that winter months will be colder than summer
102 months. The loss of predictability on a weekly time-scale arises from physical instabilities in
103 the atmospheric circulation (Lorenz, 1963), and decades of observations have allowed
104 scientists to make general statements about the temporal and spatial scales associated with
105 these instabilities, improving predictability (Bauer et al., 2015).

106 Unfortunately, we do not have enough observations of ice sheet behaviour to make
107 similar statements about the spatial and temporal scales associated with glaciological
108 variability. Ice streams are a good example; the Kamb Ice Stream shut down in the past two
109 centuries (Retzlaff and Bentley, 1993), and a myriad of ice streams with similar potential
110 behaviour have been identified from the geological record in North America and Europe
111 (Stokes and Clark, 1999; Margold et al., 2015). Modelling has shown that ice streams can be
112 generated by, for example, instabilities in thermo-mechanical coupling (Hindmarsh, 2009),
113 but none of these models have been used to match the extent of specific ice streams, due in
114 part or largely to lack of data. Another example, most likely with greater spatial extent, is the
115 marine ice sheet instability (MISI, Schoof, 2007), which acts on marine ice sheets with
116 grounding lines on reverse slopes. Both ice streams and the MISI can be viewed as examples
117 of ice sheet ‘weather’ – lack of predictability caused by instabilities, in exactly the same way
118 as atmospheric weather is generated by instabilities.

119 This leads to a conundrum increasingly faced by geologists and geomorphologists; is
120 the unusual behaviour frequently observed a signal from the whole ice sheet, or is it a signal
121 of local variability? This is where modellers can inform field scientists, since modelling can
122 give physically-based estimates of the spatial and temporal scale of unstable behaviour.

123 To account for the above limitations and uncertainties of modelled-reconstructions, two
124 general approaches have been adopted which produce multiple ice sheet simulations. The
125 first involves sensitivity analyses (e.g. Boulton and Hagdorn, 2006; Patton et al., 2016),
126 whereby relevant model parameters and boundary conditions are perturbed to produce
127 numerous simulations of the palaeo-ice sheet in question. Such tuning is conducted until a
128 simulation is generated that is perceived to ‘best fit’ the empirical evidence, and is chosen as

129 the modelled reconstruction. The second adopts an ensemble approach (e.g. Tarasov and
130 Peltier, 2004; Gregoire et al., 2012), whereby a wide set of plausible combinations of
131 parameters are input into the ice sheet model to produce an array of model-outputs. Data-
132 based constraints may then be used to rule out unrealistic simulations from the bank of
133 ensemble simulations, leaving a combination of simulations that are yet to be ruled out (e.g.
134 Gregoire et al., 2016). The second approach is to calibrate ensemble parameters against data
135 constraints, ruling out simulations and their associated parameter sets based on acceptable fits
136 to the data (e.g. Tarasov and Peltier, 2004). The remaining simulations are then supplemented
137 by further simulations, which use the calibrated parameters. The final modelled
138 reconstruction in this approach is a combination of calibrated model simulations, from which
139 the distribution of plausible glaciological variables can be derived (e.g. mean ice velocity)
140 (Tarasov et al., 2012).

141 Ideally, palaeo-ice sheet reconstructions should combine the data-rich empirical
142 approach with physically-based modelled reconstructions. Indeed, this suggestion was put
143 forward in a landmark paper by Andrews (1982), when numerical modelling was very much
144 in its infancy, and yet it has been very difficult to achieve. Ice sheet model outputs are often
145 compared to RSL data through GIA modelling (e.g. Simpson et al., 2009; Kuchar et al., 2012;
146 Auriac et al., 2016; Patton et al., 2017), but quantitative model-data comparison using other
147 forms of palaeo-ice sheet data has remained rare (although see Briggs and Tarasov, 2013;
148 Patton et al., 2016). This is despite the development (Napieralski et al., 2006; Li et al., 2007)
149 and demonstration (Napieralski et al., 2007) of tools for data-model comparison.

150 Adopting this approach may create new opportunities for both empiricists and ice sheet
151 modellers to drive the field forward. Empiricists could use models to help reduce data
152 uncertainty and rule out physically-implausible interpretations. Modellers could use the data
153 to score ensemble members and improve model formulation (as per Tarasov and Peltier,
154 2004). Here, we extend some recent advances in this area to outline a procedure for
155 comparing geochronological and geomorphological data with ice sheet model output. We
156 illustrate this with example model output of the British-Irish Ice Sheet (BIIS). Given the
157 expanding body of data constraining palaeo-ice sheet behaviour (e.g. Greenwood and Clark,
158 2009; Hughes et al., 2014; Small et al., 2017a; Clark et al., 2018), it is one of the best ice
159 sheets for model-data comparison. The primary purpose of the model runs presented here is
160 not to simulate the intricacies of this palaeo-ice sheet or advance our understanding of the ice
161 sheet, but simply to facilitate methodological comparisons between model output and

162 empirical data. Meaningful and more accurate simulations of the ice sheet are the subject of
163 ongoing work as part of the BRITICE-CHRONO NERC consortium project (e.g. Gandy et
164 al., 2018).

165 **2. Methods of model-data comparison**

166 Of the four sources of data that might be used to constrain palaeo-ice sheet simulations
167 (RSL, sedimentology, geochronology, and geomorphology), it is perhaps not surprising that
168 RSL has the longest tradition (Walcott, 1972; Peltier et al., 1978; Quinlan and Beaumont,
169 1982). Sea-level index points provide a testable dataset with definable uncertainty (e.g.
170 Engelhart and Horton, 2012). Furthermore, until recently, ice sheet models were run at a low-
171 resolution of >20 km grid size. This meant that modelled reconstructions could be tested
172 against relative-sea level data, which has a lack of abrupt spatial changes, through the use of a
173 GIA model (e.g. Auriac et al., 2016). The advent of faster and parallel processing means that
174 higher-resolution simulations of continental ice sheets are now achievable (~5 km),
175 permitting comparison to other sources of information. However, these data need to be
176 presented at a similar resolution to the model and will perhaps provide definitive and
177 quantifiable characteristics that a model can predict. Ice sheet models are yet to have
178 adequate sediment production, transportation, and deposition laws to make predictions to the
179 same level of detail that might be observed in a sediment exposure. We here demonstrate how
180 to make meaningful model-data comparisons to the remaining two classes of palaeo-ice sheet
181 data, geomorphological (ice-margin position and ice-flow direction) and geochronological (in
182 essence, the timing of ice-free conditions).

183 *2.1. Ice-Margin Position*

184 Mapping of moraines underpins empirical palaeo-glaciology, providing information on
185 former ice margin position, the direction of ice sheet retreat, and the shape of the margin
186 (Figure 1A; Clark et al., 2012). Palaeo-ice sheet models can also predict these characteristics
187 of a margin through time. However, only the largest moraines are likely to be of a sufficient
188 scale to permit meaningful comparison with ice sheet model output. To compensate for this,
189 neighbouring morainic ridges are often grouped/interpreted into larger composite margin
190 positions, which collectively delineate ice margin retreat patterns (e.g. Figure 1B).

191 Napieralski et al. (2006) developed an Automated Proximity and Conformity Analysis
192 (APCA) tool for comparing margin positions from mapped moraines and ice sheet model
193 outputs (Table 1), later modified by Li et al. (2008). In this tool, mapped margins are first

194 coarsened to conform to the ice sheet model grid size. Then, for each model-output time-
195 slice, APCA measures the distance of an ice-margin determined based on mapped moraines
196 to the modelled ice-margin (Figure 1C). The conformity of shape between margin positions
197 determined from moraines and the model output is defined as the standard deviation of
198 proximity for each cell occupied by a mapped margin position (Li et al., 2008; Figure 1C).
199 An ideal simulation of a palaeo-ice sheet would match the location and shape of each
200 moraine, which would be quantified by APCA as simultaneous zero proximity and perfect
201 conformity at some point during the model run. However, model resolution limitations mean
202 that a perfect score is unlikely to occur. Consequently, a more pragmatic approach would be
203 to apply a proximity and conformity threshold, below which an acceptable level of model-
204 data agreement occurs (Figure 1D). Only when both measures are below this predetermined
205 acceptance threshold will model-data agreement be declared, i.e. the model matches the
206 location and shape of the mapped margin derived from mapped moraines sufficiently. Where
207 the relative sequence of moraine formation is known (e.g. in a retreat sequence of concentric
208 moraines), the timing of margin matching could be considered. However, caution should be
209 taken if relative timing of moraine formation criteria are utilised, in order that simulations
210 which produce readvances that reoccupy margin positions are not excluded.

211 *2.2. Ice-flow direction*

212 Subglacial bedforms record the ice-flow directions within a palaeo-ice sheet (e.g.
213 Kleman, 1990; Clark, 1993; Kleman and Borgström, 1996; Stokes et al., 2009; Ely et al.,
214 2016). Where cross-cutting subglacial bedforms are superimposed on each other, a sequence
215 of flow directions is recorded (Clark, 1993). Neighbouring subglacial bedforms with a similar
216 morphology and orientation can be grouped into flowsets – groups of subglacial bedforms
217 interpreted to form in the same phase of ice-flow (e.g. Kleman and Borgström, 1996; Clark,
218 1999). When grouped in this way, cross-cutting flowsets of subglacial bedforms can reveal
219 major shifts in the flow patterns of an ice sheet, a consequence of shifting ice sheet geometry,
220 ice-divide migration and ice-stream (de)activation (e.g. Boulton and Clark, 1990; Clark,
221 1999; Greenwood and Clark, 2009). Whilst a single flowset provides a spatially limited
222 constraint on ice-flow direction, the sequence and spatial patterning of flowsets across the
223 former ice sheet bed can be used to reconstruct the ice-flow geometry of a palaeo-ice sheet
224 and the evolution of that geometry through time (Boulton and Clark, 1990; Kleman et al.,
225 1997; Greenwood and Clark, 2009; Hughes et al., 2014).

226 Li et al. (2007) developed an Automated Flow Direction Analysis (AFDA) tool for
227 comparing modelled and empirically derived ice sheet flow directions. To measure flow
228 correspondence, AFDA calculates the mean residual angle and variance of offset between
229 modelled and empirically derived ice-flow directions (Figure 2). Where detailed flowset
230 reconstructions exist (e.g. for the BIIS; Greenwood and Clark, 2009; Hughes et al., 2014), the
231 relative age of cross-cutting flowsets can be used as a further constraint by evaluating
232 whether a model run recreates a cross-cutting sequence of flow directions in the inferred
233 order of time (Figure 2). To do this, flow-direction model agreement would need to have
234 occurred in the specified order, beneath a predetermined (user-specified) threshold which
235 corresponds to an acceptable level of model-data agreement (Figure 2B).

236 *2.3. Ice-free timing*

237 The timing of ice-free conditions can be derived from geochronological techniques.
238 These have been applied most commonly to organic material in the case of radiocarbon
239 dating (Libby et al., 1949; Arnold and Libby, 1951; Ó Cofaigh and Evans, 2007; McCabe et
240 al., 2007), proglacial sands in the case of luminescence dating (e.g. Duller, 2006; Smedley et
241 al., 2017; Bateman et al., 2018), and glacially transported boulders or glacially modified
242 bedrock in the case of cosmogenic nuclide dating (Stone et al., 2003; Fabel et al., 2012; Small
243 et al., 2017b). For some palaeo-ice sheets, compilations of thousands of dates recording ice-
244 free conditions relevant to the timing of advance and retreat exist (Dyke, 2004; Hughes et al.,
245 2016; Small et al., 2017a). However, dating the activity of an ice sheet is complex and, as
246 such, not all dates are equally reliable constraints (Small et al., 2017a). To account for this, an
247 assessment of data reliability, such as the traffic-light system proposed by Small et al.
248 (2017a), should be conducted prior to model-data comparison. This involves initially filtering
249 out ages irrelevant to the study period. The remaining ages are then assigned a quality rating
250 based upon the stratigraphic and geomorphological context, supporting evidence and
251 potential for significant and unquantifiable geological uncertainty (Small et al. 2017a).
252 Depending on the stratigraphic setting of a dated sample (e.g. above or below glacial
253 sediment), this timing constrains ice free conditions either prior to an advance of, or
254 following the retreat of, an ice sheet (Hughes et al., 2011). Each site has an associated error,
255 related to measurement uncertainties. Since geochronological techniques only record the
256 timing of ice-free conditions prior to (advance) or after (retreat) the occupation of an area by
257 an ice sheet, the associated error can be considered as one-sided (Figure 3; Briggs and
258 Tarasov, 2013; Ely et al., in press).

259 Ely et al. (in press) developed an Automated Timing Accordance Tool (ATAT) for
260 comparing ice sheet model output with geochronological data. Ice-free dates must first be
261 grouped as constraints on the retreat or advance of the ice sheet and then gridded (rasterised)
262 to the resolution of the ice sheet model (Figure 3). Loose constraints, for example ice-free
263 dates that are thousands of years younger or older than those indicated by the regional
264 advance or retreat chronologies, can be ignored when creating the geochronological grid
265 because they provide a poor test of the ice sheet model. ATAT produces several statistics
266 based on the agreement between ice-free ages and modelled deglacial chronologies. It
267 categorises dates as to whether there is agreement within both model and data uncertainty,
268 including a procedure that considers whether a dated site could have become ice-free due to
269 thinning of the ice sheet surface (i.e. nunataks or emergent hills close to margins). After
270 classifying dates, ATAT calculates the route-mean square error (RMSE) between measured
271 and modelled ice-free timings, with an additional weighted statistic which accounts for the
272 uneven spatial distribution of dates (wRMSE). ATAT therefore measures both the number of
273 dates that agree with a simulation (% of dates that agree), and how close the simulation gets
274 to replicating the dates (wRMSE). Ideally, the ice sheet model would simulate ice-free
275 conditions within the error of each geochronological constraint. Given the limitations of
276 models, and the uncertainty associated with geochronological dates, the statistics generated
277 by ATAT can be used more pragmatically to distinguish which model-runs better conform to
278 the available geochronological archive (Ely et al., in press). For example, Ely et al. (in press)
279 suggest that the measure “number of ice-free dates agreed with within error” is a good
280 indicator from which to initially sift model simulations. A further application of ATAT is
281 demonstrated in this paper.

282 **3. Demonstration of approach using the British-Irish Ice Sheet.**

283 *3.1. Model-setup*

284 Our primary aim is to demonstrate various approaches to model-data comparison, and
285 so we perform some simple experiments with the aim of creating a range of outputs. We
286 therefore make numerous simplifications, especially regarding our climate input. It is
287 unimportant for the model experiments to exactly replicate the detailed reconstructed history
288 of the BIIS (e.g. Clark et al., 2012). However, the model output serves as a means for
289 demonstrating how model-data comparison tools could work. We use the Parallel Ice Sheet
290 Model (PISM; Winkelmann et al., 2011) to simulate the BIIS. PISM is a hybrid shallow-ice

291 shallow-shelf model which implements grounding line migration using a subgrid
292 interpolation scheme. Ice movement is modelled as a combination of ice deformation and
293 basal sliding. Internal deformation is determined by a flow law (Glen, 1952; Nye, 1953) with
294 ice rheology altered by an enthalpy scheme (Aschwanden et al., 2012). Basal sliding occurs
295 through a pseudo-plastic sliding law once basal shear stresses exceed yield stresses. Yield
296 stress is determined to be a function of till friction, with till friction being a function of
297 elevation and modelled basal effective pressure (Martin et al., 2011). Effective pressure is
298 determined by a local subglacial hydrology model which relates overburden pressure to
299 subglacial melt rates whilst ignoring horizontal water transport (Tulaczyk et al., 2000; Bueler
300 and van Pelt, 2015). The model allows ice-shelves to form. Sub-shelf melt is determined
301 using the parameterisation of Beckmann and Goosse (2003) perturbed by a melt factor
302 (Martin et al., 2011), assuming that basal ice temperature is at pressure-melting point and
303 ocean temperatures are at the freezing point at the depth of the ice-ocean interface (Martin et
304 al., 2011). Calving rates are proportional to horizontal strain rates and are determined by a 2D
305 parameterisation (Levermann et al., 2012; see also Supplementary Table 1 for key
306 parameters).

307 We run the model at 5 km resolution, using bed topography gridded from the General
308 Bathymetric Chart of the Oceans (www.gebco.net; Weatherall et al., 2015). Though higher
309 resolution simulations of palaeo-ice sheets are possible (e.g. Seguinot et al., 2018), they are
310 computationally expensive, limiting the ability to run ensembles or sensitivity analyses.
311 Furthermore, larger palaeo-ice sheets (e.g. the Laurentide), where similar approaches could
312 be conducted, require similar or coarser resolutions. Topography is updated to account for
313 isostasy using a parameterisation of viscoelastic Earth deformation in response to loading
314 (Bueler et al., 2007). Eustatic sea level change is accounted for by applying a scalar offset
315 from the SPECMAP data (Imbrie et al., 1984).

316 To demonstrate differences between model simulations, we limit our analyses to the
317 output from three model simulations. Parameters and boundary conditions are the same for all
318 three simulations, with the exception that we vary the climate input. Climate is represented in
319 our simulation as a spatially continuous field derived from multiple regression analysis of
320 three sources of climate data; two modern day records and one from a palaeo-climate
321 modelling experiment (Table 2; Braconnot et al. 2012). Prescribed temperatures are perturbed
322 over time by a scalar offset derived from the Greenland ice core records (Seierstad et al.,
323 2014) and fed into a positive degree day model to calculate surface mass balance (Calov and

324 Greve, 2005). Precipitation is also corrected with reference to the Greenland ice core record,
325 with a 7.3% reduction in precipitation per degree Celsius decrease in temperature
326 (Huybrechts, 2002). The model runs from 40 thousand years before present (ka BP) to the
327 present day. Model output was recorded at 100-year intervals. The maximum extent of ice
328 generated by each model simulation is shown in Figure 4. As expected, none of the model
329 simulations perform well at replicating the reconstructed extent of the BIIS (e.g. Clark et al.,
330 2012; Figure 4). The inability to reach these extents is most likely a consequence of the
331 simplistic climate forcing and would therefore likely be ruled out by visual assessment alone.
332 Such visual assessment is time consuming, especially considering that an ensemble is likely
333 to produce thousands of model simulations. Furthermore, it may be that the parameters used
334 in one simulation produce a closer fit to the data than others, guiding future models. It is
335 therefore important to test model-data tools against these simulated ice sheets.

336 *3.2. Ice Margin Position*

337 We derived 189 ice margin positions from moraines reported in the BRITICE v.2
338 database (Clark et al., 2018) and compared these using APCA (Li et al., 2008) against our
339 modelled ice-margin positions (Figure 5). To determine reasonable thresholds of proximity
340 and conformity beyond which model-data agreement can be declared, we conducted
341 sensitivity analysis validated by visual inspection (Figure 5B). We found that a proximity
342 threshold of 15 km and a conformity threshold of 3 km sufficiently identified modelled ice
343 margin positions that visually agreed with the shape and location of each moraine (Figure 5B,
344 5C). These thresholds could be used in similar experimental setups. A similar proximity
345 measure (15 km) was reported by Napieralski et al. (2007). Figure 5B shows an example of a
346 margin position where data-model agreement occurred. Data-model agreement occurred
347 several times during the course of the simulation for this particular margin, as both measures
348 of proximity and conformity fell below the agreement threshold on multiple occasions
349 (Figure 5C). Marine based ice sheets, such as the BIIS, are prone to readvances (Schoof,
350 2007; Kingslake et al., 2018). The potential to readvance means that we cannot make the
351 simple assumption that moraines closer to the ice sheet centre are older, meaning that we do
352 not consider time sequences of margin occupation as a test here.

353 Table 3 shows the percentage of margins matched by each model run. The most
354 common reason for model-data mismatch was that margins were not reached by the
355 simulated ice extent, meaning that they scored too low on the proximity score of APCA. This

356 is unsurprising given that 2 out of 3 of the models do not reach the extent of all considered
357 margins (Figures 4, 5A). To test whether the model agrees with the observed shape and
358 proximity of margins that are within modelled extent, we calculated a second statistic, which
359 considered only those observed margins within the maximum extent of a given model
360 simulation (Figures 4, 5A; Table 3). This shows that each simulation has model-data
361 agreement with over 50% of the margins reached and their shape replicated by the model
362 simulation (i.e. excluding mismatches for margins that are outside the maximum extent of the
363 model simulation) (Table 3). However, direct comparisons between simulations become
364 problematic when restricting the analysis to only moraines within the maximum extent, as
365 this changes the number of data that are being compared (Table 3). We therefore created a
366 third metric, the extent of margins matched within the extent Simulation C, the simulation
367 which produced the smallest ice extent (Table 3; Figure 4).

368 3.3. *Ice-flow direction*

369 A total of 103 flowsets from Britain and Ireland were compared to our model
370 simulations using AFDA (Li et al., 2007) (Figure 6A). These were assembled from
371 Greenwood and Clark (2009) and Hughes et al. (2014) and include 32 cross cutting
372 relationships. Combined, the datasets of Greenwood and Clark (2009 and Hughes et al.
373 (2014) have over 150 flowsets. However, given the horizontal resolution of the models (5
374 km), small (<20 km wide) flowsets were excluded from the analysis (n = 39). Flowsets
375 identified as times-transgressive (i.e. formed asynchronously) were either divided into the
376 stages of formation identified by Greenwood and Clark (2009) and Hughes et al. (2014), or
377 excluded from the analysis (n = 20). Flow vectors were derived from the empirically-derived
378 depiction of a flowset, rather than individual bedforms, because the orientation of these may
379 vary on a sub-grid scale. For data-model agreement to occur, we applied a threshold of 10°
380 mean residual vector, and 0.03 in mean variance. These values were initially derived by
381 visually comparing the model and data and determining whether a modelled ice flow
382 direction was sufficiently similar to a mapped flowset. These threshold values are consistent
383 with those reported by Napieralski et al. (2007), and could be used to declare model-data
384 agreement in similar experimental setups. To get a cross-cutting relationship registered to be
385 in data-model agreement, the last occurrence of model conformity for the first flowset in a
386 sequence needs to occur before the last occurrence of model conformity for the overprinted
387 flowset.

388

389 Table 3 summarises the comparison between model output from the three Simulations
390 and the assembled flowset database (Figure 6A). Overall, model-data agreement was low,
391 with the majority of flowsets not replicated by the model simulations (Table 3). Similar to the
392 margin comparison, this is partly a consequence of the models computed ice-covered area not
393 replicating the full area covered by the BIIS (Figure 4). We therefore produced a second
394 metric that restricted the analysis to those flowsets occurring within the modelled ice-extent.
395 This was done to see if model-data mismatch was a consequence of ice-extent (in which a
396 high number of ice-covered data points would be matched), or due to model-data mismatch
397 even over the ice-covered area. However, note the caveat that this limits the ability to
398 compare between simulations owing to the changing number of data in the model-data
399 comparison. A third metric, the percentage of flowsets matched within the extent of

400 simulation C (the simulation with the smallest ice extent), allows for comparison between
401 model runs. Even when this approach is adopted, the degree of model-data agreement for
402 flowsets remains low, with simulation A being the best performing, matching 26% of
403 flowsets within the extent of simulation C (Table 3). Furthermore, no models were able to
404 replicate an observed cross-cutting relationship (Table 3). Figures 6B and C demonstrate an
405 example of a matched flowset. Here, ice flow of sufficient coherence (a variance measure) in
406 an agreed direction (vector orientation measure) is achieved toward the end of the model run
407 (Figure 6C).

408

409 *3.4. Ice-free Timing*

410 Simulated ice sheet retreat timing from the model was compared to 108 published dated
411 sites of ice sheet retreat using the ATAT (Ely et al., in press). Only sites with a green or
412 amber quality rating from the traffic light system of Small et al. (2017a) were used. This
413 means that the quality control considerations of dating techniques and stratigraphic contexts
414 were deemed to be high-quality (green) or acceptable (amber). Sites flagged with ‘caution
415 when interpreting (red)’, due to specific site or technique uncertainty, were not considered
416 here (see Figure 7A for the location of sites used). For each model run, we report the
417 percentage of dates where model-data agreement occurs (i.e. when a model recreates the ice-
418 free timing recorded by geochronological data) and a spatially weighted root-mean square
419 error (wRMSE) between data-based and model-based deglaciation timing (Ely et al., in press;
420 Table 3). These measures consider the uncertainty in model-margin timing and the vertical
421 uncertainty introduced when comparing low resolution modelled ice-surface topography to
422 geochronological data collected at a point location (Ely et al., in press).

423 Simulation B performs poorly in replicating the timing of ice-free conditions, with data-
424 model conformity occurring for only 9% of the dates (Table 3). Simulations A and C have
425 higher scores of this metric, with 41% and 89% of the dates agreeing with the modelled
426 timing of ice-free conditions, respectively (Table 3). However, these model runs also have
427 high wRMSE scores (Table 3), meaning that although ice-free conditions correctly occur,
428 they are far from the mean age recorded by the geochronological data. For example, in
429 Simulation C this indicates that although model-data agreement has occurred (i.e. the model
430 has deglaciated an area before the empirical evidence indicates ice-free conditions), the

431 timing of modelled ice-free conditions is ~2000 years earlier on average than that recorded in
432 the data. This pattern of premature deglaciation is apparent in Figure 7D.

433 **4. Discussion**

434 ***4.1. Model-data fit***

435 Integration of the empirically-based and model-based approaches of ice sheet
436 reconstruction requires tools for quantifying the degree of fit between models and data.
437 Comparisons between the varied constraints of margin position, flow direction and timing,
438 such as those conducted in Section 3, are a step towards achieving this goal. A model-based
439 reconstruction is likely to be more robust if it involves multiple (100s-1000s) model
440 simulations, rather than just the three illustrated here. However, given that none of these
441 individual simulations is likely to match every piece of available evidence the question
442 “which simulations adequately recreate the available geological data?” must be addressed. By
443 addressing this question, an investigator may be able to find the optimum model
444 reconstruction (e.g. Napieralski et al., 2007; Patton et al., 2016; Seguinot et al., 2016).
445 Alternatively, these model-data tests could be incorporated as additional calibration criteria
446 for ensemble simulations (e.g. Tarasov et al., 2012), which could potentially reduce the
447 produced uncertainty of an ensemble model reconstruction.

448 Despite only using three model runs, our comparison highlights some difficulties in
449 answering the above question. For margin positions, all models performed reasonably well,
450 matching over 50% of the margins within the modelled ice sheet extent and, in the case of
451 Simulation A, 75% (Table 3). Therefore, if looking at margin position in isolation from other
452 metrics, Simulation A would be considered the best performing model-run. Since all models
453 perform well at replicating ice-marginal positions, our results, albeit limited to a small sample
454 of three simulations, suggest that the margin metric is the least stringent test of the ice sheet
455 simulations (Table 3). One possible reason for this is that models are better at replicating
456 margin shapes and positions than other data-based characteristics. However, a second
457 interpretation is that the generalisation of margin shape to a 5 km grid removes any
458 complexity in margin shape, thus promoting conformity between model and data. Future
459 work, which considers ice sheet models and margin data at different resolutions should be
460 undertaken to examine this in more detail.

461 All three model simulations do not replicate the maximum extent of the BIIS derived
462 from observations. The maximum extent of an ice sheet is generally well known, and some of

463 these moraines record the maximum extent across different sectors of the BIIS (e.g. Bradwell
464 et al., 2008; Clark et al., 2012). Therefore, future work may adopt a procedure of testing ice
465 sheet models against only those margins derived from moraines which demark maximum
466 palaeo-ice sheet extent and glaciated continental shelf-breaks (e.g. Seguinot et al., 2016;
467 Patton et al., 2017), so as to identify simulations and glacio-climatic parameter combinations
468 which achieve a reasonable ice sheet extent, before attempting to replicate margin positions
469 occupied during ice retreat. A model which fits maximum ice extent margins in some places,
470 may be able to interpolate between these constraints in a more consistent manner than
471 empirical interpretations (e.g. Bowen et al., 1986; Clark et al., 2012; Seguinot et al., 2016;
472 Patton et al., 2017).

473 All three simulations performed poorly at replicating the flow direction recorded by
474 subglacial bedforms (Table 3). This is surprising given that the direction of many flowsets
475 appears to be governed by the subglacial topography in Britain (Hughes et al., 2014), which
476 is also likely to steer ice flow directions in numerical models that use that topography. One
477 possibility is that this is due to the coarse (5 km) resolution of our model grid. Perhaps this
478 model-data mismatch is also a consequence of the model being unable to fully replicate other
479 conditions which determine ice flow direction such as basal thermal regime, subglacial
480 hydrological conditions and the overall ice-sheet geometry (e.g. location of ice divides and
481 domes). Areas with subglacial bedforms indicate warm-based ice, where basal
482 sliding/subglacial till deformation is the dominant control upon ice-discharge. The most
483 common reason for model-data mismatch in flow direction was the low mean residual
484 variance scores. In other words, the model did not produce consistent flow-directions across
485 the entire area of the flowset. Therefore, model-data mismatch is at least partially due to the
486 model being unable to adequately simulate the dimensions of ice-streams and outlet glaciers,
487 perhaps due to simplifications of physics (Hindmarsh, 2009; Stokes and Tarasov, 2010),
488 poorly constrained patterns of basal sliding parameters (Bueler and Brown, 2009), or
489 incomplete knowledge of basal sliding (Stearns and van der Veen, 2018). Climate
490 uncertainties will also influence the ability of an ice sheet model to replicate empirically
491 derived flow directions, as these impact the overall geometry of the modelled ice sheet. Since
492 these factors are a large uncertainty in ice sheet modelling (Ritz et al., 2015; Gladstone et al.,
493 2017), flowset direction is likely to be a robust test of ice sheet models. A question remains
494 regarding how long flowing ice must occupy an area in order to produce lineated flow sets; if
495 this time is decadal (e.g. Dowling et al., 2016) rather than centennial, it indicates that flowset

496 matching is not of the highest priority for ice sheet models which typically have a lower
497 temporal resolution.

498 None of the three model simulations adequately replicated a cross-cutting relationship
499 between flowsets. Such cross-cuts can be used to decipher the geometry of a palaeo-ice sheet
500 and how it changes through time (Boulton and Clark, 1990), including factors such as ice-
501 divide migration and margin position change (e.g. Greenwood and Clark, 2009; Hughes et al.,
502 2014). This means, in addition to the problems of matching a single flow-set mentioned
503 above, deglacial climate must be adequately simulated for a cross-cuts caused by climatically
504 driven ice-divide migration to be matched. In addition to this, the model must also adequately
505 represent the internal processes which cause ice-divide migration (e.g. flow piracy, ice stream
506 initiation, saddle collapse). A further uncertainty is introduced by our ignorance of ice stream
507 dynamics and how ice stream velocity and orientation can change over centennial and even
508 decadal timescales. Given these potential difficulties at matching cross-cuts, they can be
509 thought of as an even sterner test of an ice sheet model than the number of flowsets replicated
510 alone.

511 None of the three model simulations performed well when compared to the assembled
512 database of ice-free dates (Table 3). Simulation C has agreements with many sites (Table 3),
513 but simulated deglaciation occurs thousands of years prior to the age indicated by the
514 geochronological record at many sites, suggesting that retreat occurs too early and rapidly.
515 Other modelling simulations have qualitatively demonstrated a better fit to deglacial
516 chronologies by visually comparing the pattern and timing of modelled reconstructions to
517 empirically-based reconstructions (e.g. Patton et al., 2017). However, replicating the timing
518 of ice-free conditions across an ice sheet requires adequately constraining all internal and
519 external forcings through time, as well as the interactions between the two. Therefore, our
520 approach of site-by-site comparison to modelled deglacial timing provides a more stringent
521 test of model-data fit than qualitative comparisons.

522 *4.2. An approach to measuring model-data fit*

523 As a consequence of the above complexity in model-data comparison, we suggest the
524 following pragmatic approach to reconciling empirical reconstructions and model
525 reconstructions, summarised in Figure 8. Here, the investigator starts with an ensemble of ice
526 sheet model simulations; the number of simulations considered are progressively diminished
527 in number by removing those which rank lowest against a particular metric (Figure 8). This

528 builds on the suggestion of Napieralski et al. (2007) who used APCA to rule out the majority
529 of simulations, then AFDA to further evaluate model performance. Our order of rankings
530 (Figure 8) is based upon what we ascertain from the above discussion to be progressively
531 more stringent tests of a model simulation. Indeed, the order of these rankings is likely to
532 change between users who are interested in specific aspects of a palaeo-ice sheet (e.g. more
533 weighting may be given to flowset direction if studying ice-flow patterns). An alternative is
534 to combine scores derived from the model-data comparison techniques for each simulation,
535 and then rank simulations to either heavily weight the highest scoring simulations when
536 producing a probabilistic output from an ensemble (e.g. Tarasov et al., 2012), or to rule out
537 the lowest scoring simulations. In this case, the order that tests are applied is irrelevant.

538 The original ensemble of simulations is likely to contain hundreds of members and may
539 have involved some prior tuning of parameters to broadly replicate ice sheet extent (e.g.
540 Boulton and Hagdorn, 2006). Since margin position seems a comparatively simple metric
541 with which an ice sheet model result must conform, we suggest that the first set of models to
542 be ruled out are those that perform lowest in the APCA tests against margins (Napieralski et
543 al., 2006; Li et al., 2008; Figure 8). The top-performing simulations are then compared to
544 timing through the ATAT tool (Ely et al., in press; Figure 8). ATAT will produce statistics on
545 the number of dated positions matched, and how close overall the simulation gets to
546 replicating the timing of ice-free conditions (wRMSE). Thresholds of acceptance should be
547 applied for each, so that only simulations that replicate an adequate number of dates within a
548 reasonable time window from the data will remain in the ‘not-ruled out’ category of
549 simulations (Figure 8). This will rule out simulations which perform badly at replicating the
550 timing and rate of palaeo-ice sheet retreat recorded in geochronological data. Since flowset
551 conformity is likely to be a demanding test of ice sheet models, with the ability to produce
552 cross cutting flow even more demanding, we suggest remaining simulations should then be
553 ranked according to their performance according to the AFDA (Li et al., 2007; Figure 8).

554 After the application of these tests, the original ensemble of simulations will be much
555 reduced, to a set which are yet to be ruled out (Figure 8). Given that it is unlikely that a
556 perfect score will be found in these models, model-data mismatch between ‘best-fit’ models
557 should be further investigated. It may be that certain areas of empirical evidence consistently
558 produce model-data mismatch, and this may motivate further simulations if spatial or
559 temporal patterns are clear. For example, a climate driver may under-represent a particular
560 stadial, thereby producing a simulated timing which is disagrees with data. On the other hand,

561 if all surrounding empirical evidence is met, and a particular data point or subset of data
562 cannot be replicated by the model, this may warrant re-evaluation of the data in question
563 (Figure 8). In an analogous manner to climate modelling (Collins et al., 2017), it remains
564 open as to whether all models which pass a threshold acceptance barrier should be
565 incorporated into an acceptable set of reconstructions (i.e. a model democracy; Knutti, 2010)
566 or whether a “best-fit” model which performs best against all constraints should be identified
567 and used for further research. In either case, the procedure outlined above can help reduce
568 model uncertainty and produce more robust palaeo-ice sheet reconstructions.

569 *4.3. Suggestions for future developments*

570 The model-data comparison conducted here has highlighted some areas where
571 comparison tools and procedures require further development. Some required developments
572 are listed below and may aid in the reduction of both model and data uncertainty.

573 When comparing modelled and empirically derived margins using APCA, the occupied
574 side of a moraine is not considered. In situations where ice-flow geometry is likely to be
575 simple, for example in a deep trough or at the continental shelf break, this is unlikely to
576 matter. However, in more complex settings, for example where two ice sheets converge such
577 as in the North Sea, this may introduce false positives whereby a mapped margin is recorded
578 to be matched by ice flowing from the wrong direction. Our margin comparison was also
579 conducted throughout both the advance and retreat of the ice sheet. Again, this may introduce
580 false positives, as moraines known to have formed in retreat may be matched during ice
581 advance. We therefore suggest that future adaptations of APCA should consider ice flow
582 direction and the trajectory of the modelled ice margin (advance or retreat). For the latter, this
583 is unlikely to be as simple as restricting analysis to a certain time period from which
584 deglaciation commences, as maximum extents may be asynchronous (e.g. Patton et al., 2016;
585 Seguinot et al., 2018) and readvances may occur (e.g. Kingslake et al., 2018). Future work
586 should also consider penalising a model for extending beyond a well-known limit of ice-
587 extent (i.e. producing an ice-sheet that is too large). Furthermore, given the uncertainty of
588 data, it is worth considering how certain the origin of each moraine system is when applying
589 these tools. For example, could a moraine have formed during ice advance, and been
590 preserved beneath cold-based ice?

591 For ice-flow direction comparison, our analysis shows that a key problem is replicating
592 the synchronous flow directions recorded in some flowsets, and whether the model resolves

593 the timescales involved in bedform formation. Given that there is some evidence that
594 drumlins can form rapidly (Dowling et al., 2016) and the pattern of drumlins within a flowset
595 can evolve with time (Ely et al., 2018), another way of extracting more information from a
596 model-data comparison would be to compare the direction of individual bedforms to
597 modelled-flow directions. If neighbouring bedforms match within a reasonable time
598 difference, then the model could be used to classify bedforms into flowsets that could then be
599 compared to those which are empirically derived (e.g. Greenwood and Clark, 2009; Hughes
600 et al., 2014). Interpolating directions between modelled time-slices may also help improve
601 model-data comparison of flow direction, potentially capturing the flow direction of some
602 bedforms which form between model output timesteps.

603 Although influenced by overall ice sheet geometry, both margin and flow-direction are
604 predominantly constraints upon the horizontal dimension of an ice sheet. Given that the
605 thickness of ice is a vital variable for determining sea-level contribution and impacts upon the
606 landscape, vertical constraints are also important. As stated above, our comparison would
607 ideally be conducted alongside the use of a GIA model which compares to RSL data (e.g.
608 Kuchar et al., 2012; Auriac et al., 2016; Patton et al., 2017). ATAT also has a procedure for
609 identifying whether an ice-free date is positioned higher than the modelled ice-elevation (Ely
610 et al., in press), for example if a nunatak is predicted. Given the importance of these vertical
611 constraints on ice-sheet geometry, perhaps future comparisons should isolate these data as a
612 separate test of model performance.

613 **5. Summary**

614 Progress toward an integration of empirically-based and numerical model-based
615 reconstructions of palaeo-ice sheets have proven to be slow since being first suggested
616 (Andrews, 1982; Stokes et al., 2015). Here, we have outlined a procedure of model-data
617 comparison designed to score the degree of fit between ice sheet model simulations and
618 palaeo-ice sheet data, which aims to further integrate these two approaches. We compared
619 three ice sheet model simulations against the three data constraints of margin position (from
620 moraines), flow direction (from subglacial bedforms) and timing of ice-free conditions (from
621 geochronological data). In doing so, we highlighted the complexities of such model-data
622 comparisons. As ice sheet models are unlikely to reproduce all the information provided at
623 each constraint, we pragmatically suggest a hierarchical system for scoring ice sheet models,
624 whereby successive tests are applied to the ice sheet model, progressively ruling out model

625 runs which perform the poorest against each constraint. This procedure could be used to
626 ascertain best-fit models or used to calibrate models. Future work could consider in more
627 depth the relative importance of the different data-based constraints. Furthermore, we argue
628 that this approach could lead to models more frequently being used to test the plausibility of
629 data-interpretations. In future work, this comparison should ideally be made in conjunction
630 with other data-based constraints such as RSL data through GIA modelling and
631 sedimentological observations. In this manner, an integration of empirical and model-based
632 approaches to palaeo-ice sheet reconstruction can occur. The BIIS is a data rich environment
633 for conducting such model-data integration.

634

635 **Acknowledgements**

636 This work was supported by the Natural Environment Research Council (NERC) consortium
637 grant; BRITICE-CHRONO NE/J009768/1. J.C.E. acknowledges support from a NERC
638 independent research fellowship (NE/R014574/1). Development of PISM is supported by
639 NASA grant NNX17AG65G and NSF grants PLR-1603799 and PLR-1644277. We thank
640 Arjen Stroeven for editing this manuscript, as well as Irina Rogozhina and an anonymous
641 reviewer for their insightful comments.

642 **References**

- 643 Andrews, J.T., 1982. On the reconstruction of Pleistocene ice sheets: A review. *Quaternary*
644 *Science Reviews*, 1(1), pp.1-30.
- 645 Arnold, J.R. and Libby, W.F., 1951. Radiocarbon dates. *Science*, 113(2927), pp.111-120.
- 646 Aschwanden, A., Bueller, E., Khroulev, C. and Blatter, H., 2012. An enthalpy formulation for
647 glaciers and ice sheets. *Journal of Glaciology*, 58(209), pp.441-457.
- 648 Auriac, A., Whitehouse, P.L., Bentley, M.J., Patton, H., Lloyd, J.M. and Hubbard, A., 2016.
649 Glacial isostatic adjustment associated with the Barents Sea ice sheet: a modelling
650 inter-comparison. *Quaternary Science Reviews*, 147, pp.122-135.
- 651 Bateman, M.D., Evans, D.J., Roberts, D.H., Medialdea, A., Ely, J. and Clark, C.D., 2018. The
652 timing and consequences of the blockage of the Humber Gap by the last British– Irish
653 Ice Sheet. *Boreas*, 47(1), pp.41-61.
- 654 Bauer, P., Thorpe, A. and Brunet, G., 2015. The quiet revolution of numerical weather
655 prediction. *Nature*, 525(7567), p.47-55.
- 656 Beckmann, A. and Goosse, H., 2003. A parameterization of ice shelf–ocean interaction for
657 climate models. *Ocean modelling*, 5(2), pp.157-170.

- 658 Benetti, S., Dunlop, P. and Cofaigh, C.Ó., 2010. Glacial and glacially-related features on the
659 continental margin of northwest Ireland mapped from marine geophysical data. *Journal*
660 *of Maps*, 6(1), pp.14-29.
- 661 Boulton, G.S. and Clark, C.D., 1990. A highly mobile Laurentide ice sheet revealed by
662 satellite images of glacial lineations. *Nature*, 346(6287), p.813.
- 663 Boulton, G. and Hagdorn, M., 2006. Glaciology of the British Isles Ice Sheet during the last
664 glacial cycle: form, flow, streams and lobes. *Quaternary Science Reviews*, 25(23-24),
665 pp.3359-3390.
- 666 Bowen, D.Q., Rose, J., McCabe, A.M., Sutherland, D.G., 1986. Correlation of Quaternary
667 glaciations in England, Ireland, Scotland and Wales. *Quaternary Science Reviews* 5,
668 pp. 299-340
- 669 Bradley, S.L., Milne, G.A., Shennan, I. and Edwards, R., 2011. An improved glacial isostatic
670 adjustment model for the British Isles. *Journal of Quaternary Science*, 26(5), pp.541-
671 552.
- 672 Bradwell, T., Stoker, M.S., Golledge, N.R., Wilson, C.K., Merritt, J.W., Long, D., Everest,
673 J.D., Hestvik, O.B., Stevenson, A.G., Hubbard, A.L. Finlayson, A.G., and Mathers,
674 H.E., 2008. The northern sector of the last British Ice Sheet: maximum extent and
675 demise. *Earth-Science Reviews*, 88(3-4), pp.207-226.
- 676 Braconnot, P., Harrison, S.P., Kageyama, M., Bartlein, P.J., Masson-Delmotte, V., Abe-
677 Ouchi, A., Otto-Bliesner, B. and Zhao, Y., 2012. Evaluation of climate models using
678 palaeoclimatic data. *Nature Climate Change*, 2(6), p.417.
- 679 Briggs, R.D. and Tarasov, L., 2013. How to evaluate model-derived deglaciation
680 chronologies: a case study using Antarctica. *Quaternary Science Reviews*, 63, pp.109-
681 127.
- 682 Bueler, E.D., Lingle, C.S. and Brown, J., 2007. Fast computation of a viscoelastic deformable
683 Earth model for ice sheet simulations. *Annals of Glaciology*, 46(1), pp.97-105.
- 684 Bueler, E. and Brown, J., 2009. Shallow shelf approximation as a “sliding law” in a
685 thermomechanically coupled ice sheet model. *Journal of Geophysical Research: Earth*
686 *Surface*, 114(F3).
- 687 Bueler, E. and Pelt, W.V., 2015. Mass-conserving subglacial hydrology in the Parallel Ice
688 Sheet Model version 0.6. *Geoscientific Model Development*, 8(6), pp.1613-1635.
- 689 Calov, R. and Greve, R., 2005. A semi-analytical solution for the positive degree-day model
690 with stochastic temperature variations. *Journal of Glaciology*, 51(172), pp.173-175.
- 691 Clark, C.D., 1993. Mega-scale glacial lineations and cross-cutting ice-flow landforms. *Earth*
692 *surface processes and landforms*, 18(1), pp.1-29.
- 693 Clark, C.D., 1999. Glaciodynamic context of subglacial bedform generation and
694 preservation. *Annals of Glaciology*, 28, pp.23-32.

- 695 Clark, C.D., Hughes, A.L., Greenwood, S.L., Jordan, C. and Sejrup, H.P., 2012. Pattern and
696 timing of retreat of the last British-Irish Ice Sheet. *Quaternary Science Reviews*, 44,
697 pp.112-146.
- 698 Clark, C.D., Ely, J.C., Greenwood, S.L., Hughes, A.L., Meehan, R., Barr, I.D., Bateman,
699 M.D., Bradwell, T., Doole, J., Evans, D.J. Jordan, C.J., Moneys, X., Pellicer, M. and
700 Sheehy, M., 2018. BRITICE Glacial Map, version 2: a map and GIS database of glacial
701 landforms of the last British–Irish Ice Sheet. *Boreas*, 47(1), p.11.
- 702 Collins, M., 2017. Still weighting to break the model democracy. *Geophysical Research*
703 *Letters*, 44(7), pp.3328-3329.
- 704 Dowling, T.P., Möller, P. and Spagnolo, M., 2016. Rapid subglacial streamlined bedform
705 formation at a calving bay margin. *Journal of Quaternary Science*, 31(8), pp.879-892.
- 706 Duller, G.A.T., 2006. Single grain optical dating of glacial deposits. *Quaternary*
707 *Geochronology*, 1(4), pp.296-304.
- 708 Dyke, A.S., 2004. An outline of North American deglaciation with emphasis on central and
709 northern Canada. *Developments in Quaternary Sciences*, 2, pp.373-424
- 710 Ely, J.C., Clark, C.D., Spagnolo, M., Stokes, C.R., Greenwood, S.L., Hughes, A.L., Dunlop,
711 P. and Hess, D., 2016. Do subglacial bedforms comprise a size and shape
712 continuum?. *Geomorphology*, 257, pp.108-119.
- 713 Ely, J.C., Clark, C.D., Spagnolo, M., Hughes, A.L. and Stokes, C.R., 2018. Using the size
714 and position of drumlins to understand how they grow, interact and evolve. *Earth*
715 *Surface Processes and Landforms*, 43(5), pp.1073-1087.
- 716 Ely, J.C., Clark, C.D., Small, D., Hindmarsh, R.C.A, in press. ATAT 1.1, an Automated
717 Timing Accordance Tool for comparing ice sheet model output with geochronological
718 data. *Geoscientific Model Development Discussions*.
- 719 Engelhart, S.E. and Horton, B.P., 2012. Holocene sea level database for the Atlantic coast of
720 the United States. *Quaternary Science Reviews*, 54, pp.12-25.
- 721 Eyles, N. and McCabe, A.M., 1989. The Late Devensian (< 22,000 BP) Irish Sea Basin: the
722 sedimentary record of a collapsed ice sheet margin. *Quaternary Science Reviews*, 8(4),
723 pp.307-351.
- 724 Fabel, D., Ballantyne, C.K. and Xu, S., 2012. Trimlines, blockfields, mountain-top erratics
725 and the vertical dimensions of the last British–Irish Ice Sheet in NW
726 Scotland. *Quaternary Science Reviews*, 55, pp.91-102.
- 727 Fisher, D., Reeh, N. and Langley, K., 1985. Objective reconstructions of the late Wisconsinan
728 Laurentide Ice Sheet and the significance of deformable beds. *Géographie physique et*
729 *Quaternaire*, 39(3), pp.229-238.
- 730 Gandy, N., Gregoire, L.J., Ely, J.C., Clark, C.D., Hodgson, D.M., Lee, V., Bradwell, T. and
731 Ivanovic, R.F., 2018. Marine ice sheet instability and ice shelf buttressing of the Minch
732 Ice Stream, northwest Scotland. *The Cryosphere*, 12(11), pp.3635-3651.

- 733 Gladstone, R.M., Warner, R.C., Galton-Fenzi, B.K., Gagliardini, O., Zwinger, T. and Greve,
734 R., 2017. Marine ice sheet model performance depends on basal sliding physics and
735 sub-shelf melting. *The Cryosphere*, 11(1), p.319.
- 736 Glen, J.W., 1952. Experiments on the deformation of ice. *Journal of Glaciology*, 2(12),
737 pp.111-114.
- 738 Greenwood, S.L. and Clark, C.D., 2009. Reconstructing the last Irish Ice Sheet 2: a
739 geomorphologically-driven model of ice sheet growth, retreat and
740 dynamics. *Quaternary Science Reviews*, 28(27-28), pp.3101-3123.
- 741 Gregoire, L.J., Payne, A.J. and Valdes, P.J., 2012. Deglacial rapid sea level rises caused by
742 ice sheet saddle collapses. *Nature*, 487(7406), p.219.
- 743 Gregoire, L.J., Otto-Bliesner, B., Valdes, P.J. and Ivanovic, R., 2016. Abrupt Bølling
744 warming and ice saddle collapse contributions to the Meltwater Pulse 1a rapid sea level
745 rise. *Geophysical research letters*, 43(17), pp.9130-9137.
- 746 Herbertson, A.J. (1908). *Outlines of Physiography: An Introduction to the Study of the Earth*.
747 Edward Arnold, London. 3rd ed. Page 118.
- 748 Hindmarsh, R.C., 2009. Consistent generation of ice-streams via thermo-viscous instabilities
749 modulated by membrane stresses. *Geophysical Research Letters*, 36(6).
- 750 Hubbard, A., Bradwell, T., Golledge, N., Hall, A., Patton, H., Sugden, D., Cooper, R. and
751 Stoker, M., 2009. Dynamic cycles, ice streams and their impact on the extent,
752 chronology and deglaciation of the British–Irish ice sheet. *Quaternary Science*
753 *Reviews*, 28(7), pp.758-776.
- 754 Hughes, A.L., Greenwood, S.L. and Clark, C.D., 2011. Dating constraints on the last British-
755 Irish Ice Sheet: a map and database. *Journal of Maps*, 7(1), pp.156-184.
- 756 Hughes, A.L., Clark, C.D. and Jordan, C.J., 2014. Flow-pattern evolution of the last British
757 Ice Sheet. *Quaternary Science Reviews*, 89, pp.148-168.
- 758 Hughes, A.L., Gyllencreutz, R., Lohne, Ø.S., Mangerud, J. and Svendsen, J.I., 2016. The last
759 Eurasian ice sheets—a chronological database and time-slice reconstruction, DATED-
760 1. *Boreas*, 45(1), pp.1-45.
- 761 Hughes, T., 1973. Is the West Antarctic ice sheet disintegrating?. *Journal of Geophysical*
762 *Research*, 78(33), pp.7884-7910.
- 763 Huybrechts, P., 2002. Sea-level changes at the LGM from ice-dynamic reconstructions of the
764 Greenland and Antarctic ice sheets during the glacial cycles. *Quaternary Science*
765 *Reviews*, 21(1-3), pp.203-231.
- 766 Imbrie, J., Hays, J.D., Martinson, D.G., McIntyre, A., Mix, A.C., Morley, J.J., Pisias, N.G.,
767 Prell, W.L. and Shackleton, N.J., 1984. The orbital theory of Pleistocene climate:
768 support from a revised chronology of the marine $\delta^{18}\text{O}$ record. In A. L. Berger, J.
769 Imbrie, J. Hays, G. Kukla, & B. Saltzman (Eds.), *Milankovitch and climate* (pp. 269–
770 305). Dordrecht, Holland: Milankovitch and Climate.

771 Kingslake, J., Scherer, R.P., Albrecht, T., Coenen, J., Powell, R.D., Reese, R., Stansell, N.D.,
772 Tulaczyk, S., Wearing, M.G. and Whitehouse, P.L., 2018. Extensive retreat and re-
773 advance of the West Antarctic ice sheet during the Holocene. *Nature*, 558(7710), p.430.

774 Kleman, J., 1990. On the use of glacial striae for reconstruction of paleo-ice sheet flow
775 patterns: with application to the Scandinavian ice sheet. *Geografiska Annaler: Series A,*
776 *Physical Geography*, 72(3-4), pp.217-236.

777 Kleman, J. and Borgström, I., 1996. Reconstruction of palaeo-ice sheets: the use of
778 geomorphological data. *Earth surface processes and landforms*, 21(10), pp.893-909.

779 Kleman, J., Hättestrand, C., Borgström, I. and Stroeven, A., 1997. Fennoscandian
780 palaeoglaciology reconstructed using a glacial geological inversion model. *Journal of*
781 *glaciology*, 43(144), pp.283-299.

782 Knutti, R., 2010. The end of model democracy? *Climatic Change*, 102, 395-404.

783 Kuchar, J., Milne, G., Hubbard, A., Patton, H., Bradley, S., Shennan, I. and Edwards, R.,
784 2012. Evaluation of a numerical model of the British–Irish ice sheet using relative sea-
785 level data: implications for the interpretation of trimline observations. *Journal of*
786 *Quaternary Science*, 27(6), pp.597-605.

787 Lambeck, K. and Chappell, J., 2001. Sea level change through the last glacial
788 cycle. *Science*, 292(5517), pp.679-686.

789 Levermann, A., Albrecht, T., Winkelmann, R., Martin, M.A., Haseloff, M. and Joughin, I.,
790 2012. Kinematic first-order calving law implies potential for abrupt ice-shelf
791 retreat. *The Cryosphere*, 6, pp.273-286.

792 Li, Y., Napieralski, J., Harbor, J. and Hubbard, A., 2007. Identifying patterns of
793 correspondence between modeled flow directions and field evidence: an automated
794 flow direction analysis. *Computers & geosciences*, 33(2), pp.141-150.

795 Li, Y., Napieralski, J. and Harbor, J., 2008. A revised automated proximity and conformity
796 analysis method to compare predicted and observed spatial boundaries of geologic
797 phenomena. *Computers & Geosciences*, 34(12), pp.1806-1814.

798 Libby, W.F., Anderson, E.C. and Arnold, J.R., 1949. Age determination by radiocarbon
799 content: world-wide assay of natural radiocarbon. *Science*, 109(2827), pp.227-228.

800 Lorenz, E.N., 1963. Deterministic nonperiodic flow. *Journal of the Atmospheric*
801 *Sciences*, 20(2), pp.130-141.

802 Margold, M., Stokes, C.R. and Clark, C.D., 2015. Ice streams in the Laurentide Ice Sheet:
803 Identification, characteristics and comparison to modern ice sheets. *Earth-Science*
804 *Reviews*, 143, pp.117-146.

805 Martin, M.A., Winkelmann, R., Haseloff, M., Albrecht, T., Bueller, E., Khroulev, C. and
806 Levermann, A., 2011. The Potsdam Parallel Ice Sheet Model (PISM-PIK)—Part 2:
807 Dynamic equilibrium simulation of the Antarctic ice sheet. *The Cryosphere*, 5(3),
808 pp.727-740.

- 809 McCabe, A.M., Clark, P.U., Clark, J. and Dunlop, P., 2007. Radiocarbon constraints on
810 readvances of the British–Irish Ice Sheet in the northern Irish Sea Basin during the last
811 deglaciation. *Quaternary Science Reviews*, 26(9-10), pp.1204-1211
- 812 Napieralski, J., Li, Y. and Harbor, J., 2006. Comparing predicted and observed spatial
813 boundaries of geologic phenomena: Automated Proximity and Conformity Analysis
814 applied to ice sheet reconstructions. *Computers & geosciences*, 32(1), pp.124-134.
- 815 Napieralski, J., Hubbard, A., Li, Y., Harbor, J., Stroeven, A.P., Kleman, J., Alm, G. and
816 Jansson, K.N., 2007. Towards a GIS assessment of numerical ice sheet model
817 performance using geomorphological data. *Journal of Glaciology*, 53(180), pp.71-83.
- 818 Nye, J.F., 1953. The flow law of ice from measurements in glacier tunnels, laboratory
819 experiments and the Jungfraufirn borehole experiment. *Proc. R. Soc. Lond.*
820 *A*, 219(1139), pp.477-489.
- 821 Ó Cofaigh, C. and Evans, D.J., 2007. Radiocarbon constraints on the age of the maximum
822 advance of the British–Irish Ice Sheet in the Celtic Sea. *Quaternary Science*
823 *Reviews*, 26(9-10), pp.1197-1203.
- 824 Patton, H., Hubbard, A., Andreassen, K., Winsborrow, M. and Stroeven, A.P., 2016. The
825 build-up, configuration, and dynamical sensitivity of the Eurasian ice sheet complex to
826 Late Weichselian climatic and oceanic forcing. *Quaternary Science Reviews*, 153,
827 pp.97-121.
- 828 Patton, H., Hubbard, A., Andreassen, K., Auriac, A., Whitehouse, P.L., Stroeven, A.P.,
829 Shackleton, C., Winsborrow, M., Heyman, J. and Hall, A.M., 2017. Deglaciation of the
830 Eurasian ice sheet complex. *Quaternary Science Reviews*, 169, pp.148-172.
- 831 Peltier, W.R., 2004. Global glacial isostasy and the surface of the ice-age Earth: the ICE-5G
832 (VM2) model and GRACE. *Annu. Rev. Earth Planet. Sci.*, 32, pp.111-149.
- 833 Peltier, W.R., Farrell, W.E. and Clark, J.A., 1978. Glacial isostasy and relative sea level: a
834 global finite element model. *Tectonophysics*, 50(2-3), pp.81-110.
- 835 Piotrowski, J.A. and Tulaczyk, S., 1999. Subglacial conditions under the last ice sheet in
836 northwest Germany: ice-bed separation and enhanced basal sliding?. *Quaternary*
837 *Science Reviews*, 18(6), pp.737-751.
- 838 Quinlan, G. and Beaumont, C., 1982. The deglaciation of Atlantic Canada as reconstructed
839 from the postglacial relative sea-level record. *Canadian Journal of Earth*
840 *Sciences*, 19(12), pp.2232-2246.
- 841 Retzlaff, R. and Bentley, C.R., 1993. Timing of stagnation of Ice Stream C, West Antarctica,
842 from short-pulse radar studies of buried surface crevasses. *Journal of*
843 *Glaciology*, 39(133), pp.553-561.
- 844 Ritz, C., Edwards, T.L., Durand, G., Payne, A.J., Peyaud, V. and Hindmarsh, R.C., 2015.
845 Potential sea-level rise from Antarctic ice sheet instability constrained by
846 observations. *Nature*, 528(7580), pp.115-118.

- 847 Schoof, C., 2007. Ice sheet grounding line dynamics: Steady states, stability, and
848 hysteresis. *Journal of Geophysical Research: Earth Surface*, 112(F3).
- 849 Schoof, C., 2012. Marine ice sheet stability. *Journal of Fluid Mechanics*, 698, pp.62-72.
- 850 Seierstad, I.K., Abbott, P.M., Bigler, M., Blunier, T., Bourne, A.J., Brook, E., Buchardt, S.L.,
851 Buizert, C., Clausen, H.B., Cook, E. Dahl-Jensen, D., Davies, S.M., Guillevic, M.,
852 Johnsen, S.J., Pedersen, D.S., Popp, T.J., Rasmussen, S.O., Severinghaus, J.P.,
853 Svensson, A. and Vinther, B.M., 2014. Consistently dated records from the Greenland
854 GRIP, GISP2 and NGRIP ice cores for the past 104 ka reveal regional millennial-scale
855 $\delta^{18}\text{O}$ gradients with possible Heinrich event imprint. *Quaternary Science*
856 *Reviews*, 106, pp.29-46.
- 857 Seguinot, J., Khroulev, C., Rogozhina, I., Stroeven, A.P. and Zhang, Q., 2014. The effect of
858 climate forcing on numerical simulations of the Cordilleran ice sheet at the Last Glacial
859 Maximum. *The Cryosphere*, 8(3), pp.1087-1103.
- 860 Seguinot, J., Rogozhina, I., Stroeven, A.P., Margold, M., Kleman, J., 2016. Numerical
861 simulations of the Cordilleran ice sheet through the last glacial cycle. *The Cryosphere*
862 10, pp. 639-664.
- 863 Seguinot, J., Ivy-Ochs, S., Jouvét, G., Huss, M., Funk, M. and Preusser, F., 2018. Modelling
864 last glacial cycle ice dynamics in the Alps. *The Cryosphere*, 12(10), pp.3265-3285.
- 865 Simpson, M.J., Milne, G.A., Huybrechts, P. and Long, A.J., 2009. Calibrating a glaciological
866 model of the Greenland ice sheet from the Last Glacial Maximum to present-day using
867 field observations of relative sea level and ice extent. *Quaternary Science*
868 *Reviews*, 28(17-18), pp.1631-1657.
- 869 Small, D., Clark, C.D., Chiverrell, R.C., Smedley, R.K., Bateman, M.D., Duller, G.A., Ely,
870 J.C., Fabel, D., Medialdea, A. and Moreton, S.G., 2017a. Devising quality assurance
871 procedures for assessment of legacy geochronological data relating to deglaciation of
872 the last British-Irish Ice Sheet. *Earth-science reviews*, 164, pp.232-250.
- 873 Small, D., Benetti, S., Dove, D., Ballantyne, C.K., Fabel, D., Clark, C.D., Gheorghiu, D.M.,
874 Newall, J. and Xu, S., 2017b. Cosmogenic exposure age constraints on deglaciation and
875 flow behaviour of a marine-based ice stream in western Scotland, 21–16
876 ka. *Quaternary Science Reviews*, 167, pp.30-46.
- 877 Smedley, R.K., Scourse, J.D., Small, D., Hiemstra, J.F., Duller, G.A.T., Bateman, M.D.,
878 Burke, M.J., Chiverrell, R.C., Clark, C.D., Davies, S.M. Fabel, D., Gheorghiu, D.M.,
879 McCarroll, D., Medialdea, A., and Xu S., 2017. New age constraints for the limit of the
880 British–Irish Ice Sheet on the Isles of Scilly. *Journal of Quaternary Science*, 32(1),
881 pp.48-62
- 882 Stearns, L.A. and van der Veen, C.J., 2018. Friction at the bed does not control fast glacier
883 flow. *Science*, p.eaat2217.
- 884 Stokes, C.R. and Clark, C.D., 1999. Geomorphological criteria for identifying Pleistocene ice
885 streams. *Annals of glaciology*, 28, pp.67-74.

- 886 Stokes, C.R. and Tarasov, L., 2010. Ice streaming in the Laurentide Ice Sheet: A first
887 comparison between data-calibrated numerical model output and geological
888 evidence. *Geophysical Research Letters*, 37(L01501).
- 889 Stokes, C.R., Clark, C.D. and Storrar, R., 2009. Major changes in ice stream dynamics during
890 deglaciation of the north-western margin of the Laurentide Ice Sheet. *Quaternary*
891 *Science Reviews*, 28(7-8), pp.721-738.
- 892 Stokes, C.R., Tarasov, L., Blomdin, R., Cronin, T.M., Fisher, T.G., Gyllencreutz, R.,
893 Hättestrand, C., Heyman, J., Hindmarsh, R.C., Hughes, A.L., Jakobsson, M., Kirchner,
894 N., Livingstone, S.J., Margold, M., Murton, J.B., Noormets, R., Peltier, R.W., Peteet,
895 D.M., Piper, D.J.W., Preusser, F., Renssen, H., Roberts, D.H., Roche, D.M., Saint-
896 Ange, F., Stroeven, A.P. and Teller, J.T., 2015. On the reconstruction of palaeo-ice
897 sheets: recent advances and future challenges. *Quaternary Science Reviews*, 125, pp.15-
898 49.
- 899 Stone, J.O., Balco, G.A., Sugden, D.E., Caffee, M.W., Sass, L.C., Cowderly, S.G. and
900 Siddoway, C., 2003. Holocene deglaciation of Marie Byrd land, west
901 Antarctica. *Science*, 299(5603), pp.99-102.
- 902 Stroeven, A.P., Hättestrand, C., Kleman, J., Heyman, J., Fabel, D., Fredin, O., Goodfellow,
903 B.W., Harbor, J.M., Jansen, J.D., Olsen, L., Caffee, M.W., Fink, D., Lundqvist, J.,
904 Rosqvist, G.C., Strömberg, B. and Jansson, K.N., 2016. Deglaciation of
905 Fennoscandia. *Quaternary Science Reviews*, 147, pp.91-121.
- 906 Tarasov, L. and Peltier, W.R., 2004. A geophysically constrained large ensemble analysis of
907 the deglacial history of the North American ice sheet complex. *Quaternary Science*
908 *Reviews*, 23(3-4), pp.359-388.
- 909 Tarasov, L., Dyke, A.S., Neal, R.M. and Peltier, W.R., 2012. A data-calibrated distribution of
910 deglacial chronologies for the North American ice complex from glaciological
911 modeling. *Earth and Planetary Science Letters*, 315, pp.30-40.
- 912 Tulaczyk, S., Kamb, W.B. and Engelhardt, H.F., 2000. Basal mechanics of ice stream B,
913 West Antarctica: 1. Till mechanics. *Journal of Geophysical Research: Solid*
914 *Earth*, 105(B1), pp.463-481.
- 915 Walcott, R.I., 1972. Late Quaternary vertical movements in eastern North America:
916 Quantitative evidence of glacio- isostatic rebound. *Reviews of Geophysics*, 10(4),
917 pp.849-884.
- 918 Weatherall, P., Marks, K.M., Jakobsson, M., Schmitt, T., Tani, S., Arndt, J.E., Rovere, M.,
919 Chayes, D., Ferrini, V. and Wigley, R., 2015. A new digital bathymetric model of the
920 world's oceans. *Earth and Space Science*, 2(8), pp.331-345.
- 921 Winkelmann, R., Martin, M.A., Haseloff, M., Albrecht, T., Bueler, E., Khroulev, C. and
922 Levermann, A., 2011. The Potsdam parallel ice sheet model (PISM-PIK)-Part 1: Model
923 description. *The Cryosphere*, 5(3), p.715.

924 **Tables:**

925 Table 1 – Summary of sources of data and comparison tools discussed in this paper.

Glaciological characteristic	Model representation	Empirical data basis	BIIS data used in this study	Data-model comparison tool
Margin-position.	Extent mask or determined from ice thickness.	Moraines (or other ice-contract/marginal landforms).	189 margin positions derived from the BRITICE v.2 compilation (Clark et al., 2018; Figure 5).	Automated Proximity and Conformity Analysis (APCA) (Napieralski et al., 2006; Li et al., 2008).
Ice flow direction.	Continuous field produced by model.	Subglacial bedforms, often grouped into flowsets (distinct flow events).	103 flowsets with 32 cross-cutting relationships (Greenwood and Clark, 2009; Hughes et al., 2014; Figure 6).	Automated Flow Direction Analysis (AFDA) (Li et al., 2007)
Timing of ice-free conditions.	Change in ice sheet extent mask, or ice thickness grid to 0 metres.	Geochronological data (mainly from Terrestrial Cosmogenic Nuclide, ¹⁴ C and Optically Stimulated Luminescence dating)	108 dated sites derived from previous literature (Small et al., 2017a; Figure 7). Only sites with Green or Amber quality rating are used (see Section 2.3).	Automated Timing Accordance Tool (ATAT) (Ely et al., in press).

926

927

928 Table 2. Multiple regression fields for climate. lat = latitude, lon = longitude, topg = surface topography (i.e. elevation in metres above present-
 929 day sea-level).

Simulation	Precipitation (mm/a)	Mean Annual temperature (°C)	July temperature (°C)	Source of climate data
A	$374.6 + 10.1 \times \text{lat} - 26.0 \times \text{lon}$	$25.3 - 0.004 \times \text{topg} - 0.294 \times \text{lat} - 0.035 \times \text{lon}$	$32.2 - 0.004 \times \text{topg} - 0.316 \times \text{lat} - 0.009 \times \text{lon}$	www.worldclim.org/
B	$81.1 + 0.116 \times \text{lat} - 1.502 \times \text{lon}$	$35.8 - 0.005 \times \text{topg} - 4.97 \times \text{lat} - 0.07 \times \text{lon}$	$34.2 - 0.004 \times \text{topg} - 0.343 \times \text{lat} + 0.112 \times \text{lon}$	www.cru.uea.ac.uk/data
C	$159.8 - 16.545 \times \text{lat} - 12.342 \times \text{lon}$	$33.7 - 0.007 \times \text{topg} - 0.674 \times \text{lat} - 0.218 \times \text{lon}$	$39.358 - 0.007 \times \text{topg} - 0.621 \times \text{lat} + 0.18 \times \text{lon}$	pmip3.lsce.ipsl.fr/

930

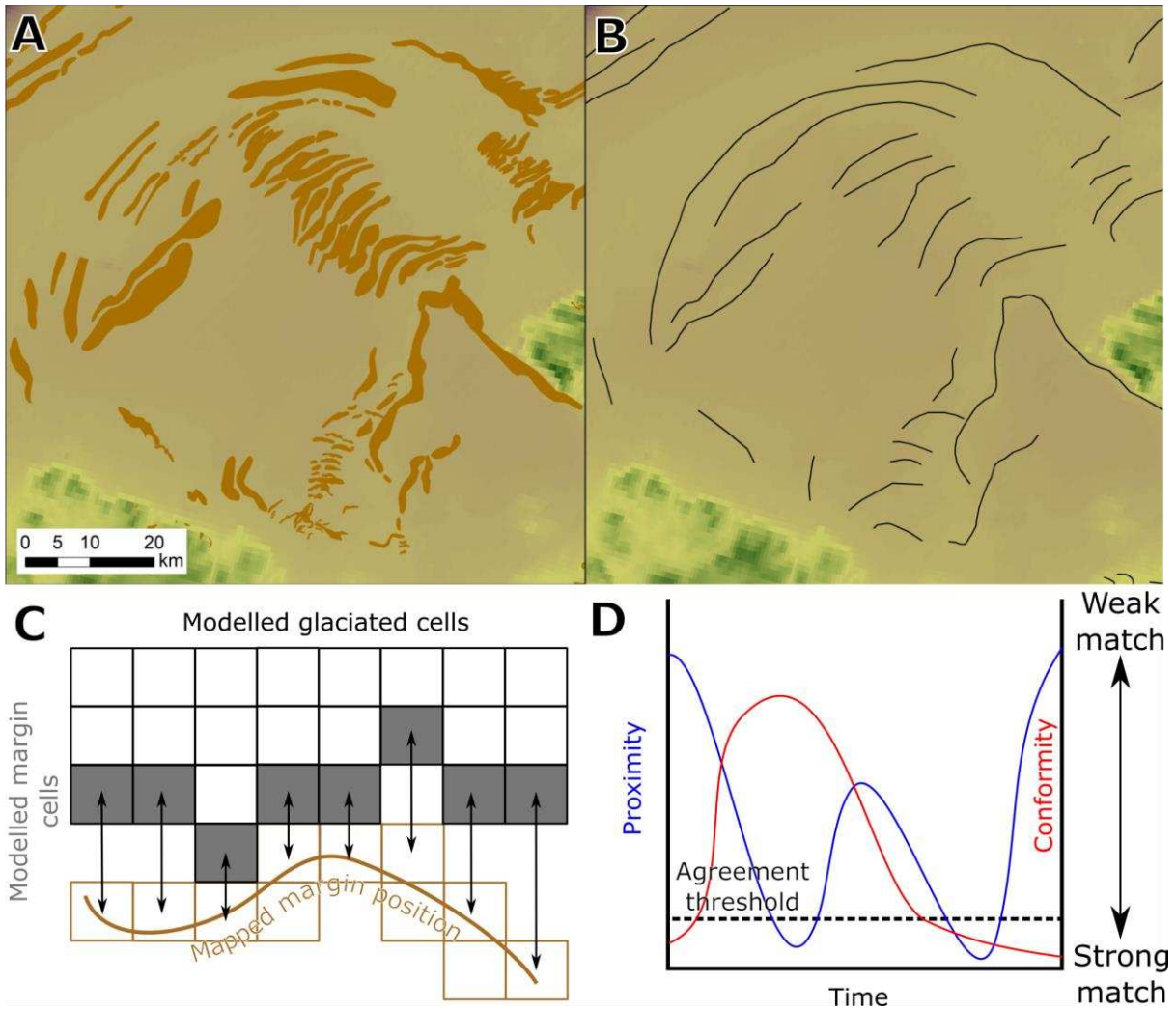
931

932 Table 3. Summary of results from model-data comparisons. Note that when measures are restricted to the modelled ice extent, the number
 933 of comparisons change, limiting the ability to compare between simulations.

	Simulation																		
A	60	% of margins matched (n = 189)	76 (n = 151)	% of margins matched within maximum modelled extent	61	% of margins matched within extent of simulation C	9	% of flowsets matched (n = 103)	21 (n = 41)	% of flowsets matched within maximum modelled extent	26	% of flowsets matched within extent of simulation C	0	% of cross-cuts matched	41	% of dates where model-data agreement occurs (n = 108)	1898	wRMSE of model-data difference for ice covered dates where model-data agreement occurs (years)	
B	36		54 (n = 125)		43		16		19 (n = 88)		21		0		9		1182		
C	43		66 (n = 124)		66		3		8 (n = 39)		8		0		89		2057		

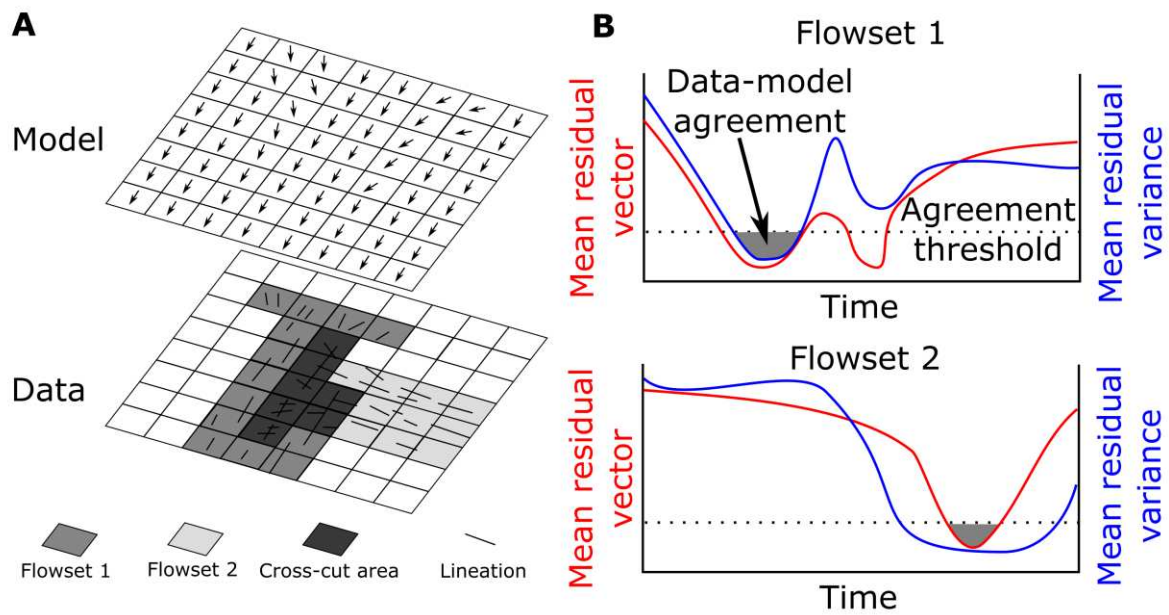
934

935



937

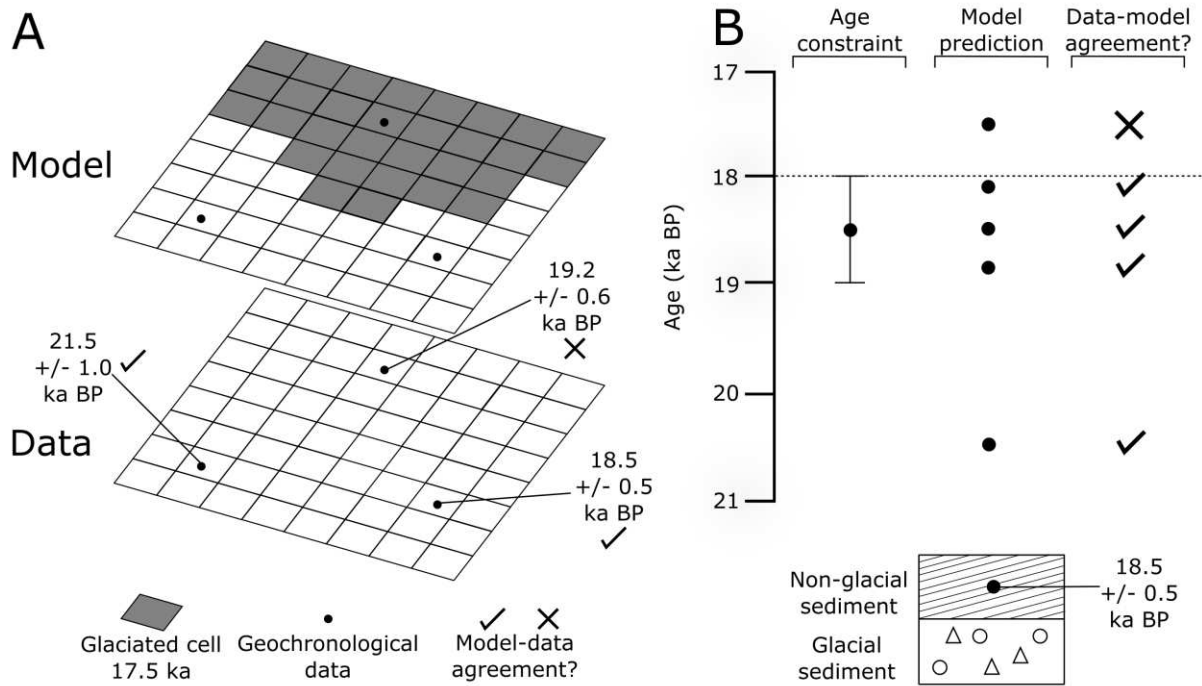
938 Figure 1. A) Mapped offshore moraines, Donegal Bay, Ireland, from Benetti et al. (2010). B)
 939 Interpreted margin positions from A. C) Schematic representation of the Automated
 940 Proximity and Conformity Analysis (APCA), whereby the distance between modelled and
 941 mapped margin position is measured. Proximity is defined as the mean of these
 942 measurements and conformity as the standard deviation (Napieralski et al., 2006; Li et al.,
 943 2008). D) Schematic output from APCA. Here, a model-data agreement is only declared
 944 when both proximity and conformity are below a defined threshold. Such instances are
 945 shaded in grey.



946

947 Figure 2. A) Schematic of Automated Flow Direction Analysis comparison technique (after
 948 Li et al., 2007). At this point in time, the model agrees well with Flowset 1, but is flowing at
 949 right angles to the superimposed Flowset 2. For complete model-data agreement to occur, the
 950 model must replicate the flow direction of flowset 2 at a later stage. B) Schematic output
 951 from AFDA for Flowsets 1 and 2 depicted in A. In this case, data-model agreement occurs
 952 when both mean residual variance and the mean residual vector are below an applied
 953 threshold. As this occurs in the observed sequence (Flowset 1 then Flowset 2), model data-
 954 agreement of this cross-cutting relationship can be said to occur.

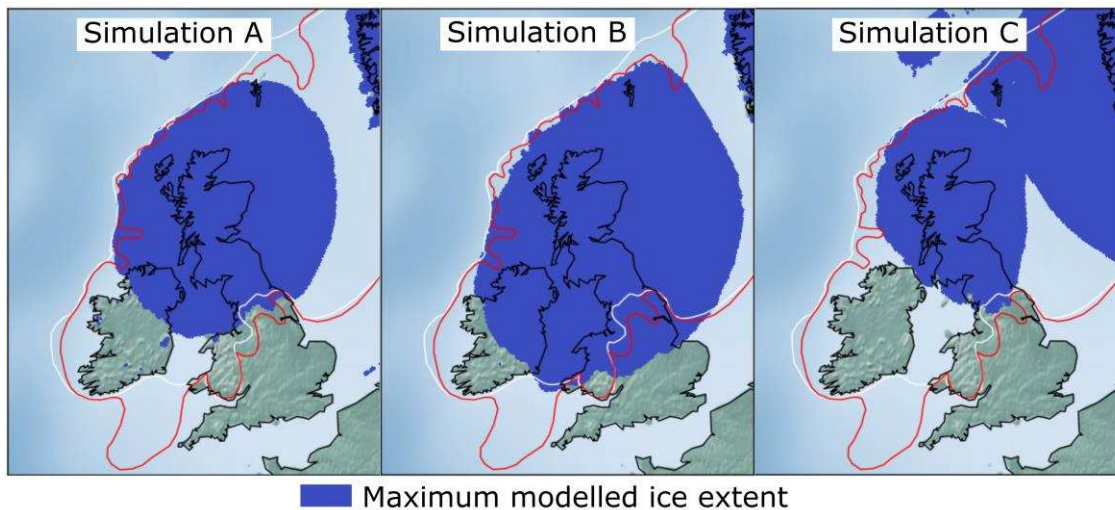
955



957

958 Figure 3. A) Schematic of the comparison between model and data made by ATAT (Ely et
 959 al., in press). Example shows a deglaciating ice sheet model output at 17.5 ka BP. The model
 960 replicates the ice-free conditions recorded by the lower two sites and thus there is model-data
 961 agreement. However, the model still produces ice cover at this time within the range of the
 962 date of 19.2 ± 0.6 ka BP. In this case, there is model-data disagreement. B) Example of
 963 comparison procedure for one site, dated to 18.5 ± 0.5 ka BP. Model predictions that occur
 964 before an ice-free age, or during the associated error, are considered to agree with the data.
 965 Adapted from Ely et al. (in press).

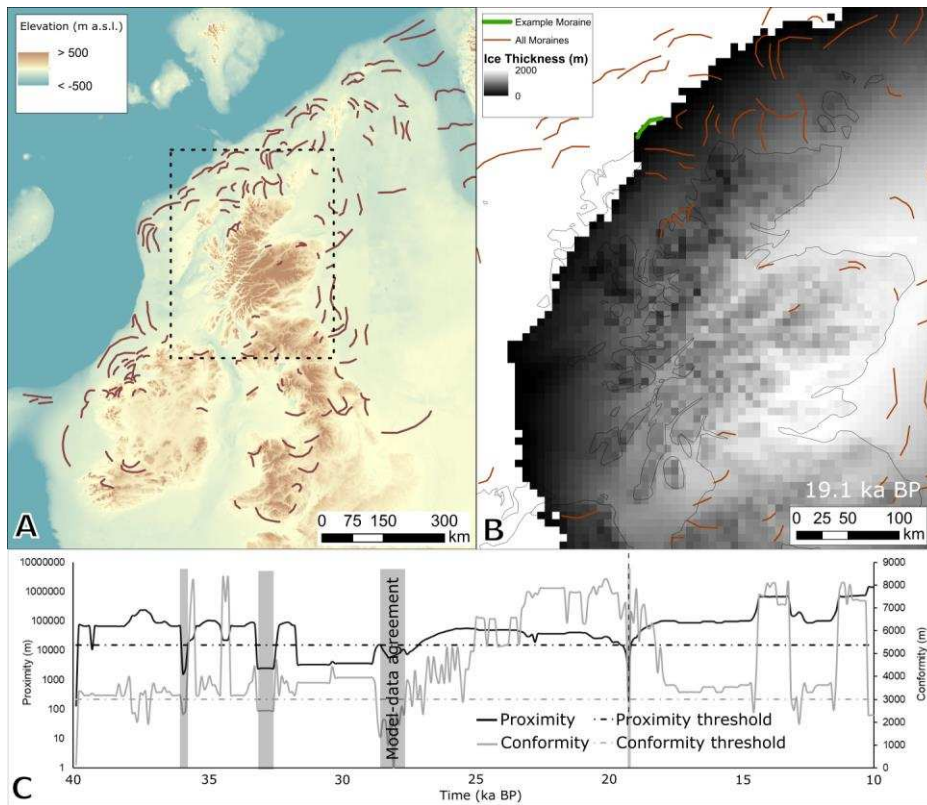
966



967

968 Figure 4. The maximum extent of the three model simulations. Note that these simulations
969 are only driven by climate and are not calibrated to any empirical evidence of the ice sheet.
970 Thus, they do not achieve a state which resembles the empirically reconstructed ice sheet.
971 Reconstructed extents at 27 ka BP (white line) and 23 ka BP from Clark et al. (2012) are
972 shown for comparison.

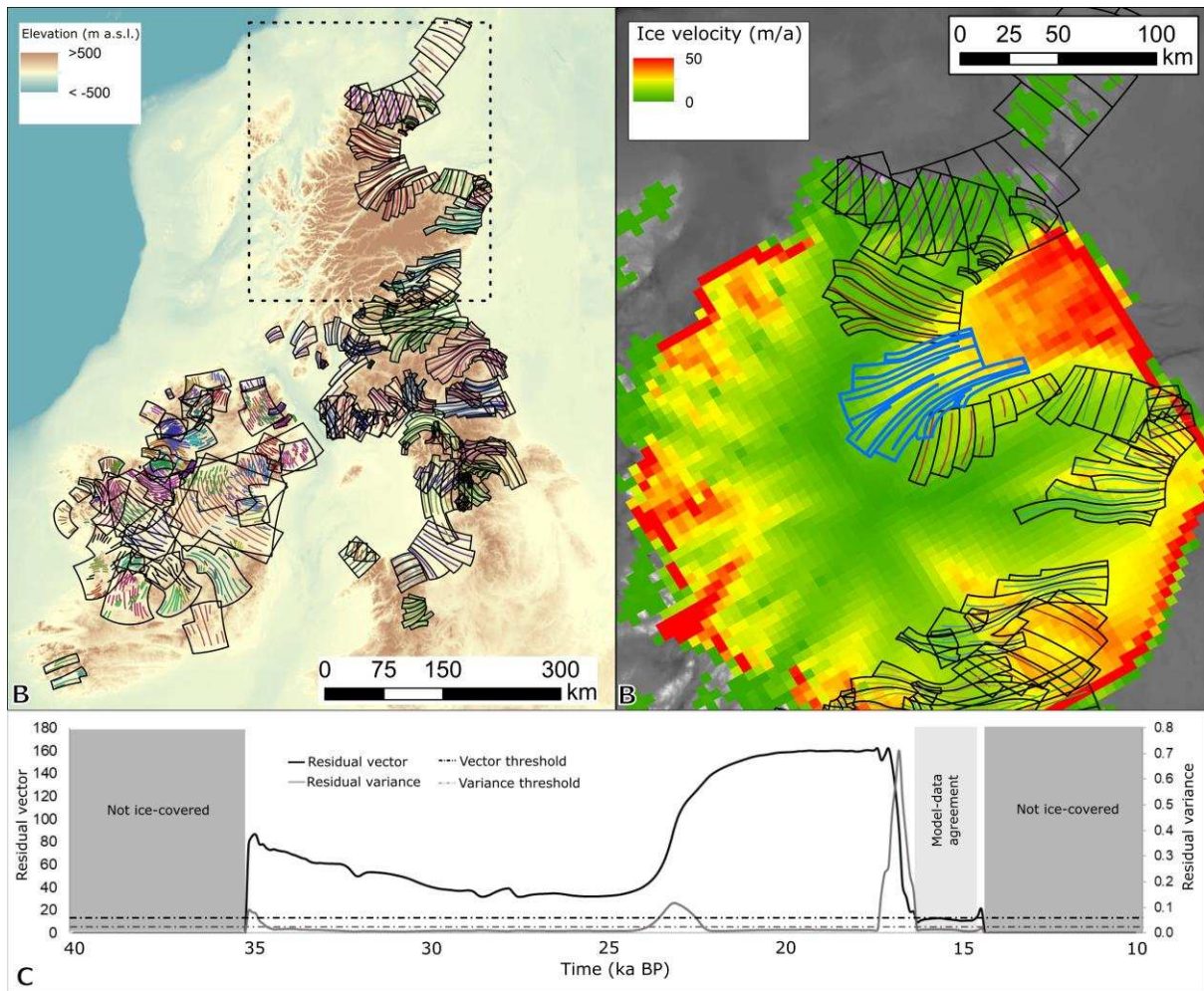
973



974

975 Figure 5. A) Generalised margin positions tested, derived from moraines reported in Clark et
 976 al. (2018). Merged bathymetry and topography from the General Bathymetric Chart of the
 977 Oceans 2014 grid (GEBCO; Weatherall et al., 2015). B) Modelled ice sheet thickness at 19.1
 978 ka BP from Simulation A, centred on north-west Scotland with ice margin positions plotted
 979 on top. The example moraine considered in panel C is highlighted in green. Location of this
 980 panel is the dashed box on panel A. C) Output of proximity and conformity analysis for the
 981 example moraine shown in B for the duration of simulation A (40 ka BP to 10 ka BP). Note
 982 there are several periods of time when both proximity and conformity indicate model-data
 983 agreement, the most recent being at 19.1 ka BP. Note that the axis for “Proximity” is
 984 logarithmic.

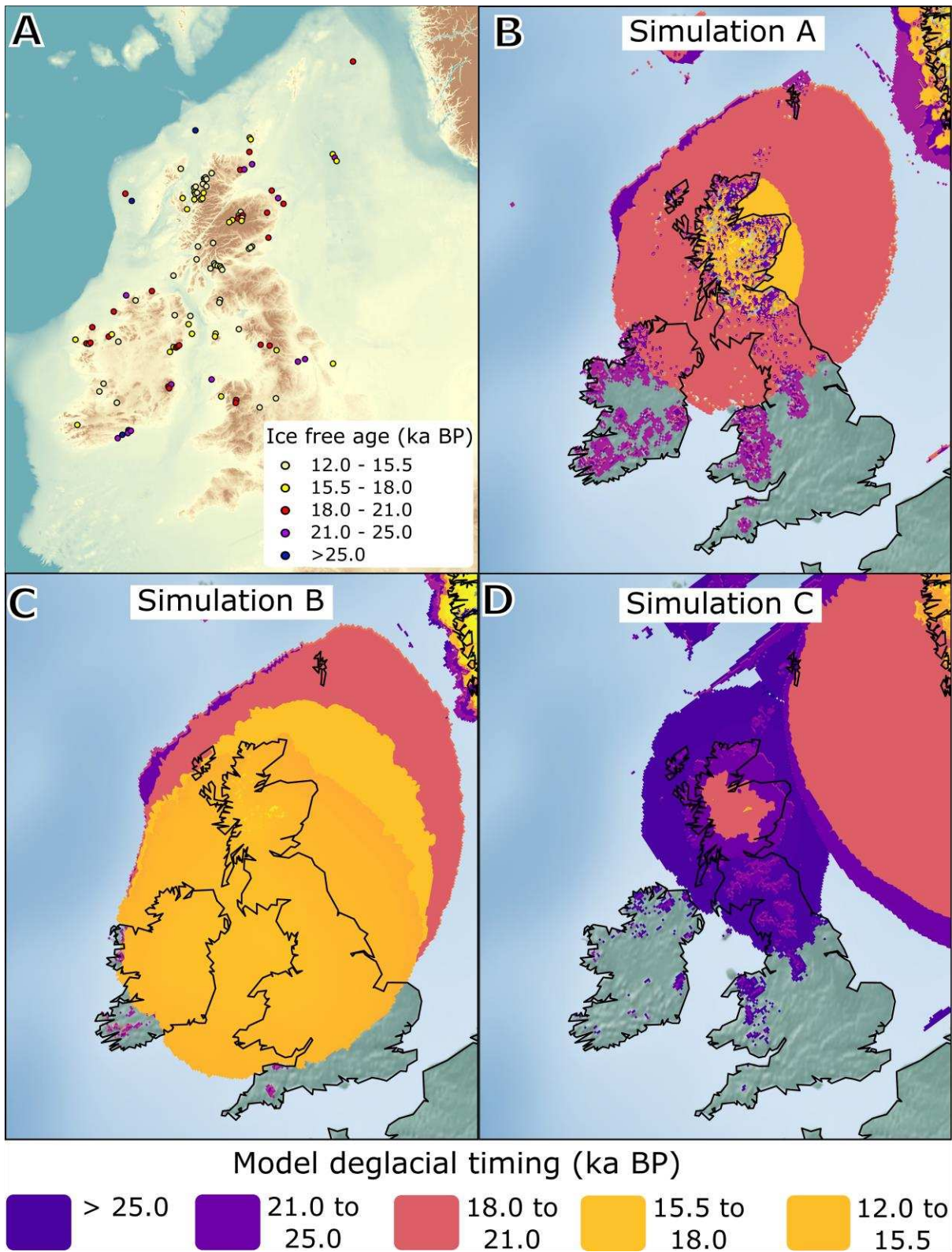
985



986

987 Figure 6. A) Flowsets used to compare to model simulations, with colours indicating different
 988 flowsets. Background from GEBCO (Weatherall et al., 2015). Overlapping regions are
 989 regions of cross-cutting (from Greenwood and Clark (2009a) and Hughes et al. (2014)). B)
 990 An example of a matched flowset, highlighted in blue, from simulation B at 17.1 ka BP.
 991 Other flowsets are indicated by coloured lines encompassed by black boxes. This panel is
 992 located by the dashed box on panel A. C) Output from AFDA for model simulation B (40 ka
 993 BP to 10 ka BP), showing periods of model-data agreement over time for the flowset shown
 994 in (B).

995



996

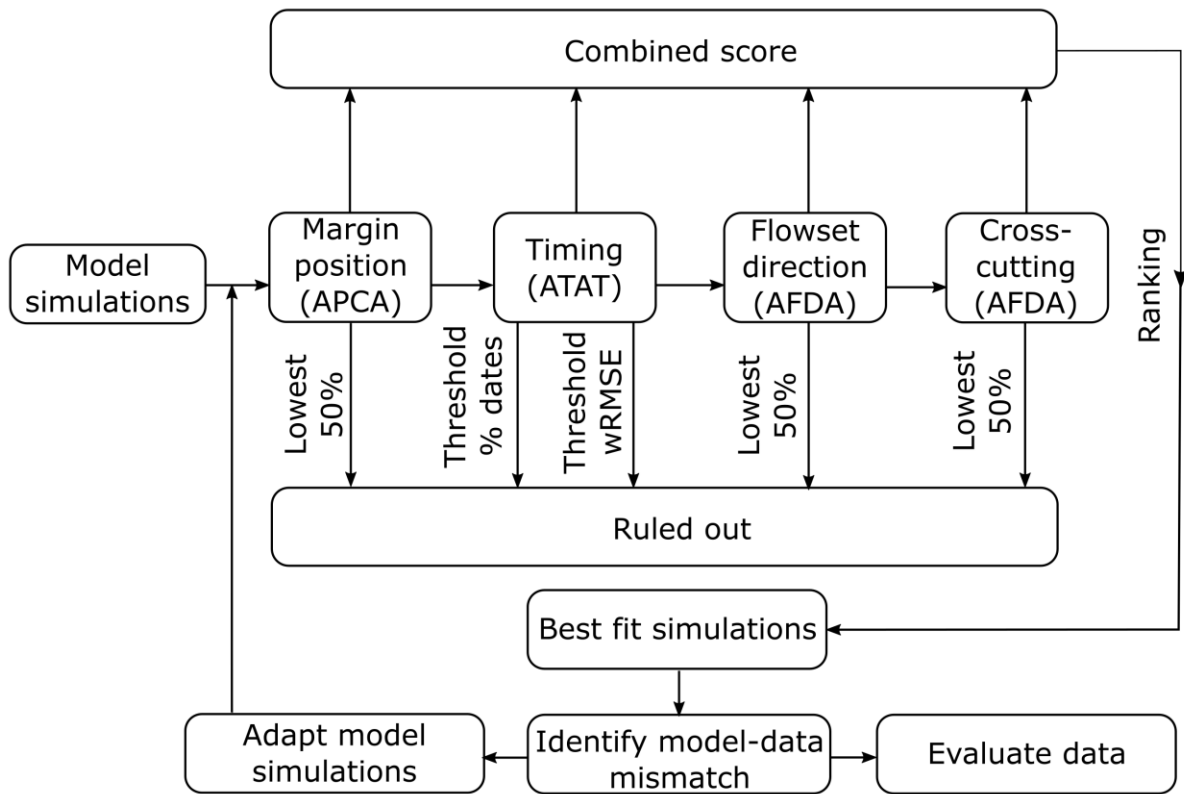
997

998

999

1000

Figure 7. A) Dated locations assembled from Small et al. (2017a) that have a quality rating of green or amber. B to D) Simulated timing of ice-free conditions from model simulations A to C. Note that these simulations are uncalibrated to any empirical evidence, and a better fit may be achieved by tuning parameters and boundary conditions.



1001

1002 Figure 8. Proposed procedure for comparing multiple model-runs to geochronological data.